

PEOPLE'S DEMOCRATIC REPUBLIC OF ALGERIA  
MINISTRY OF HIGHER EDUCATION AND SCIENTIFIC RESEARCH

*University of Mohamed El-Bashir El-Ibrahimi - Bordj Bou Arreridj*

**Faculty of Science and Technology**

*Department of Electronics*

# ***Master Thesis***

*Presented to obtain*

**THE MASTER'S DEGREE**

**FILIERE:** Electronics

**Specialty:** Telecommunications System

By:

- *Ms. Mekhalfia Boutheyna*
- *Ms. Medjdoub Amira*

*Entitled*

***Photonic Crystal Structure for Bio sensing Application.***

***Supported the: 04/07/2023.***

***Devant le Jury composé de :***

<b><i>Name</i></b>	<b><i>Grade</i></b>	<b><i>Qualité</i></b>	<b><i>Etablissement</i></b>
<b><i>M.Boutout Farid</i></b>	<b><i>Pr.</i></b>	<b><i>Président</i></b>	<b><i>Univ-BBA</i></b>
<b><i>M.Bendib Sarra</i></b>	<b><i>MCB</i></b>	<b><i>Encadreur</i></b>	<b><i>Univ-BBA</i></b>
<b><i>M. Fares.F</i></b>	<b><i>MCA</i></b>	<b><i>Examineur</i></b>	<b><i>Univ-BBA</i></b>

***Année Universitaire 2022/2023***

---

## *Acknowledgments*

*First, we wish of all to thank ﷻ the Almighty and Merciful, who gave us the strength and patience to carry out this modest work.*

*Secondly, we would like to thank our coach, **Dr. Bendib Sara**, for the orientation, the confidence, and the patience that has been a considerable memory without which this work could not have been carried out at the right port. May he find in this work a living tribute to his high personality.*

*Our sincere thanks also go to the members of **the jury** for their interest in our research by agreeing to examine our work and enrich it with their proposals. Finally, we would also like to thank all those who have been directly or indirectly involved in this work.*

## *Dedication*

*To my greatest supporters and sources of inspiration, I dedicate this work with all my infinite love and gratitude.*

*To my mother, who has always been my place of attachment and compass, thank you for your unconditional love, dedication and unwavering support . You were the light that lit my way through dark times and you always believed in me, even when I doubted.*

*To my father who taught me the importance of hard work compasss, thank you for your unconditional love, dedication, and ailing support. You inspired me to aim higher and pursue my dreams. I am infinitely grateful to you for your unwavering support, trust in me, and love.*

*To my brothers, Chaker, aymen, achref, and my sisters Maria, Nina, Mimi who are also my best friends, thank you for your constant support, your contagious humor, and your comforting presence. You are my source of joy and happiness, and I am proud to have you in my life.*

*To my very dear Soulef, khawla, and Ihssen friends, who have been my pillars in difficult times and my party partners in times of joy, thank you for your sincere friendship, your unwavering support, and your unconditional love.*

*Finally, to my binôme amira who has become a dear friend, thank you for our fruitful collaboration.*

*Beyond the names mentioned, there is a precious circle of people who have played a significant role in my journey. I express my gratitude to you for your presence and your support which have had a positive impact on my life.*

*Mekhalfia Boutheyra*

## *Dedication*

*To the one who taught me ambition.*

*To my dear parents who are paying with love and sacrifice the price for my way of thinking, they made me a woman. To my dear brothers, my friends.*

*To all those who, from far or near, have contributed to the realization of this modest work.*

*Medjdoub Amira*

# Table of Contents

Acknowledgments.

Dedication.

Dedication.

List of Figures.

List of Tables.

List equation.

Acronyms and Abbreviations.

Abstract.

General Introduction ..... 2

Bibliographic references of General Introduction ..... 3

## Chapter 01: Photonic crystal sensor.

Introduction ..... 5

State of the art ..... 5

1. Definition ..... 7

2. Basic properties of photonic crystals ..... 8

2.1. 1D Photonic Crystals (One-dimensional) ..... 8

2.2. 3D Photonic Crystals (three-dimensional) ..... 8

2.3. 2D Photonic Crystals (two-dimensional) ..... 9

2.4. Defects in 2D photonic crystals ..... 11

2.4.1. Linear defect ..... 11

2.4.2. Point defects ..... 12

3. Applications of photonic crystals ..... 13

5. Mechanism of detections ..... 14

5.1. Absorption sensing ..... 14

5.2. Fluorescence sensing ..... 15

5.3. Surface Plasmon resonance sensing ..... 15

5.4. Refractive index sensing ..... 15

5.4.1. Band gap variation: ..... 15

5.4.2. Wavelength shift sensing: ..... 15

6. Characteristic paramètres ..... 15

6.1. Sensitivity(s) ..... 15

6.2. The detection limit ..... 16

6.3. Quality factor .....	16
6.4. Figure of merit .....	16
7. Objectify .....	17
Conclusion: .....	17
Bibliographic references of Chapter 01 .....	18

## **Chapter 02: Software and the simulation method.**

Introduction .....	25
1. Modulation Methods and software .....	25
1.1. The FDTD method .....	25
1.2. The PWE method .....	26
2. OptiFDTD .....	26
2.1. Specific Benefits .....	26
2.2. Applications .....	27
2.3. OptiFDTD coordinates system .....	27
3. work on the program (optiFDTD) .....	28
3.1. OptiFDTD Designer .....	30
3.2. Profile Designer .....	31
3.3. OptiFDTD Simulator .....	32
Conclusion .....	34
Bibliographic references of Chapter 02 .....	35

## **Chapter 03: High Sensitivity Refractive Index Sensor based on a photonic crystal for the detection of chikungunya virus .**

Introduction .....	37
1. Article Structure and the Corresponding Styles .....	38
2. Geometric Study .....	42
3. Discussion and Results .....	44
Conclusions .....	48
Bibliographic references of Chapter 03 .....	49
General Conclusion .....	51
Bibliographic References of General Conclusion .....	53

## List of Figures

Figure 1 : Photonic crystals in (a) 1D, (b) 2D, and (c) 3D, D being the dimension .....	7
Figure 2 : One-dimensional periodic structure.....	8
Figure 3 : <i>The first BIP3D structure: yablonovite</i> .....	9
Figure 4 : Two-dimensional periodic structure .....	9
Figure 5 : (a) Connected 2D structure (b) Disconnected 2D structure.....	10
Figure 6 : Representation (a) of a square network (b) of a triangular network (c) of a hexagonal network.....	10
Figure 7 : Band diagram of a triangular two-dimensional photonic crystal. (My works).....	11
Figure 8 : Diagram of a faulty guide in a network (a) of columns of a dielectric (b) of air holes ].....	12
Figure 9 : Different types of defects (a) H0-cavity. (b) L3-cavity. (c) Ring resonator. (d) Hetro-structure cavity. (e) Linear waveguide. (f) Coupled-cavity waveguide .....	13
Figure 10 : Definition of a sensor.....	14
Figure 11 : Some examples of physical quantities detectable by phc means .....	14
Figure 12 : The coordinate system used in OptiFDTD. ....	27
Figure 13 : The workflow of a typical simulation using OptiFDTD.....	29
Figure 14 : OptiFDTD Designer window. ....	30
Figure 15 : Crystal lattice properties (setting of structure). ....	30
Figure 16: Profile designer (materials and profile used). ....	31
Figure 17 : profile definition window. ....	31
Figure 18 : Input field properties.....	32
Figure 19 : Setting of simulation.....	33
Figure 20 : OptiFDTD analyze and observation Area Analysis.....	33
Figure 21 : <i>Observation results and superposition curves (in colors)</i> . ....	34
Figure 22 : The proposed design.....	40
Figure 23 :The structure in 3D. ....	40
Figure 24 : The band gap of the photonic crystal structure. ....	41
Figure 25 : <i>Field distribution</i> .....	42
Figure 26 : change in the width Vs the sensitivity. ....	43
Figure 27 : The final design. ....	44
Figure 28 : Normalized transmission spectrum of healthy and infected RBC. ....	45
Figure 29 : Normalized transmission spectrum of healthy and infected Platelets.....	46
Figure 30 : Normalized transmission spectrum of healthy and infected plasma.....	46
Figure 31 : Normalized transmission spectrum of healthy and infected uric acid. ....	47

## List of Tables

Table 1 : Design Parameters.....	41
<i>Table 2 : Sensitivity value for each Parameter change.....</i>	<i>43</i>
Table 3 : Refractive index of each analyte.....	45
Table 4 : Sensitivity, effectiveness, and quality factor for each analyte.....	47
Table 5 : Comparison of Research.....	47



## Acronyms and Abbreviations

PC	Photonic Crystal
1D	One dimension
2D	Two dimensions
3D	Three dimensions
PBG	Photonic Band Gap
EBG	Electromagnetic band gap
TM	Magnetic transverse
TE	Transverse Electrical
SPR	Surface Plasmonic Resonance.
RI	Refractive index
FDTD	Domaine temporel de différence finie
PWE	Expansion des ondes planes
PWE–OPTIFDTD	Simulation software
Mid-IR	Medium infrared.
LOD	Limit of detection.
SWG	Sub Wavelength grating

## Abstract

The work presented in this thesis concerns the study and the simulation of a biosensor based on a two-dimensional photonic crystal to detect the chikungunya virus.

The simulation results have designed and analyzed by using the finite difference time domain (FDTD) method under the OptiFDTD software, the band gap calculation is performed using the plane wave expansion method (PWE) under PWE solver, and MATLAB for plotting curves. The obtained results thanks to the design that we used, are very satisfactory because they show a very high sensitivity reaching 973.24um/RIU and transmission up to 69.2%, which makes it a very good support for the realization of our biosensor.

**Keywords:** Photonic crystals, biosensor, GaAs, chikungunya virus, OptiFDTD.

## Résumé

Le travail présenté dans cette thèse concerne l'étude et la simulation d'un biocapteur basé sur un cristal photonique bidimensionnel pour détecter le virus chikungunya.

Les résultats de la simulation ont été conçus et analysés en utilisant la méthode de la différence finie dans domaine temporel (FDTD) sous le logiciel OptiFDTD, le calcul de l'écart de bande est effectué en utilisant la méthode d'expansion d'onde plane (PWE) sous le solveur PWE, et MATLAB pour tracer les courbes. Les résultats obtenus grâce au design que nous avons utilisé, sont très satisfaisants car ils montrent une sensibilité très élevée atteignant 973.24um/RIU et une transmission jusqu'à 69.2%, ce qui en fait un très bon support pour la réalisation de notre biocapteur.

**Mot clé :** cristaux photoniques, biocapteur, GaAs, virus chikungunya, OptiFDTD.

### المخلص

يتعلق العمل المقدم في هذه الأطروحة بدراسة ومحاكاة جهاز استشعار حيوي يعتمد على بلورة ضوئية ثنائية الأبعاد للكشف عن فيروس الشيكونغونيا.

تم تصميم نتائج المحاكاة وتحليلها استخدام طريقة نطاق زمن الاختلاف المحدود (FDTD) في إطار برنامج OptiFDTD، ويتم إجراء حساب فجوة النطاق باستخدام طريقة توسيع موجة الطائفة (PWE) تحت محلل PWE، واستعمال MATLAB لرسم المنحنيات. النتائج التي تم الحصول عليها بفضل التصميم الذي استخدمناه مرضية للغاية لأنها تظهر حساسية عالية جداً تصل إلى 973.24 um/RIU والانتقال حتى 69.2٪، مما يجعلها قاعدة جيدة للمضي قدماً في تصنيع جهاز الاستشعار للكشف عن فيروس الشيكونغونيا.

**الكلمات الرئيسية:** بلورات ضوئية، مستشعر حيوي، فيروس شيكونغونيا، GaAs, OptiFDTD

# **General Introduction**

## General Introduction

For many years, research has focused on the behavior of photons rather than electrons, intending to control the propagation of light, thus offering the possibility of blocking or letting through certain frequency ranges and in one or more several directions. John [1] (1987) and other scientists have created and characterized a new generation of materials: photonic crystals.

Photonic crystals (PCs) are nanostructured materials in which the refractive index varies periodically [2]. Due to the band structure and light confinement of photonic crystals, photonic crystals can be used as detection elements. These sensors allow rapid analysis of the biological interactions being sought. Due to their small size. Eventually, they may replace analytical laboratories for rapid point-of-care diagnostics.

Chikungunya virus is spread to humans through mosquito bites and is characterized by symptoms like high fever, intense joint pain, headache, muscle pain, rash, and fatigue [3].

The wide spread of the Chikungunya virus where the number of patients reached more than 210,000 in the first months of 2023 has highlighted the urgent need for the early detection of the disease to protect and treat patients and prevent future outbreaks. that is why we have simulated a 2D Photonic crystal connected structure composed of holes in a GaAs substrate Software have been used for Plane-wave expansion (PWE) and finite difference time domain (FDTD) are PWE Solver and Optifdtd respectively, and MATLAB software for plotting. In this context, this dissertation is divided into three chapters:

In the first chapter, we have reviewed the notions of photonic crystals and the basic definitions relating to these structures, to provide a photonic band gap (BIP) which represents the essential support for the realization of different types of sensors using this type of structure.

The second chapter contained general information about the program uses OptiFDTD, and the main numerical methods used to model the PHc structures.

In Chapter 3, The proposed structure has been presented and the steps that should be followed to design a 2D photonic crystal-based biosensor for the detection of chikungunya virus have been described where the OptiFDTD software and the PWE Solver.Finally, we discussed the obtained simulation results.

## **Bibliographic References**

- [1] K. Busch and S. John, ‘Liquid-Crystal Photonic-Band-Gap Materials: The Tunable Electromagnetic Vacuum’, *Phys. Rev. Lett.*, vol. 83, no. 5, pp. 967–970, Aug. 1999, doi: 10.1103/PhysRevLett.83.967.
- [2] E. Yablonovitch, ‘Photonic band-gap crystals’, *J. Phys. Condens. Matter*, vol. 5, no. 16, p. 2443, Apr. 1993, doi: 10.1088/0953-8984/5/16/004.
- [3] ‘With rising cases, experts discuss Chikungunya spread in the Americas - PAHO/WHO | Pan American Health Organization’. <https://www.paho.org/en/news/4-5-2023-rising-cases-experts-discuss-chikungunya-spread-americas> (accessed May 30, 2023).

# **Chapter 01**

## **Photonic crystal sensor**

### **Introduction**

The interest of researchers in the topic of photonic crystals is important, especially since the late 90s, because these artificial periodic materials have been promised to revolutionize the field of telecommunications and detections [1]. Indeed, for years, scientific research has believed that it can control the propagation of light thanks to these materials to replace conventional electric current communication. This would result in a huge gain in terms of speed of communication [2].

This chapter aims to present the basic concepts concerning photonic crystals, and their optical properties. A special place is given to two-dimensional crystals, state of the art, and the objective of our work.

### **State of the art**

The birth of photonic structures comes from optics. During the last decades that photonic crystals have attracted great attention, the first hypotheses on the possibility of controlling the propagation of light using periodic structures relate to 1887 with the work of Lord Rayleigh. In 1922, the English physicist sir William Lawrence Bragg developed the Bragg mirror. This mirror is a succession of transparent flat surfaces with different refractive indices. Thanks to constructive interference phenomena, it allows the reflection of 99.5% of the incident energy, which is impossible with a classic mirror. It was not until 1987 that Eli yablonovitch [3] proposed to extend the concept of Bragg mirrors to microwave frequencies for some kind of impact.

In 1991, Eli Yablonovitch made the first artificial photonic crystal operating at centimeter wavelengths. This artificial crystal is called Yablonovite [4].

In 1995, the Vasily Astratov group made a significant discovery regarding natural and synthetic opals. They found that these opals possess a characteristic known as PHc (complete photonic band gap) with an incomplete forbidden band [5].

The following year, in 1996, Thomas Kramse demonstrated the existence of PHc in 2D at a specific wavelength. This breakthrough opened up new possibilities for PHc manufacturing in semiconductor materials, particularly within the industry [6].

During the same period, Pavel Cheban introduced a waveguide called nv type (grating waveguide under  $\lambda$  (SWG)) that effectively reduced the effects of wave interference. This

waveguide was strategically designed to operate outside the forbidden band, thus minimizing wave interference [7].

Moving ahead to 1998, Philip Russell achieved a significant milestone by improving normal fiber optics and introducing photonic crystal fibers. This advancement revolutionized the field of fiber optics [8].

In 2006, researchers discovered a natural photonic crystal structure in the scales of a Brazilian beetle, marking a ground-breaking finding in the natural world [9].

Subsequently, in 2012, a diamond crystal structure was detected in a weevil [10], [11] and a gyroid-like architecture was identified in a butterfly [12]. These discoveries further expanded our understanding of photonic crystal structures and their prevalence in nature.

More recently, researchers have uncovered gyroid photonic crystals in the feather barbs of blue-winged birds. These intricate structures play a crucial role in producing the bird's captivating shimmering blue coloration.

Photonic crystals are periodic structures that can manipulate the propagation of light by creating a photonic bandgap, where certain frequencies of light are forbidden from propagating through the structure. This unique property has made them useful in a variety of applications, including bio-sensing [13].

The addition of photonic crystals to biosensors has enabled highly sensitive and specific detection of biological molecules [14]. By functionalizing the photonic crystal surface with biomolecules that selectively bind to target molecules, changes in the photonic crystal's refractive index can be detected, indicating the presence of the target molecule [15]. This allows for rapid and highly sensitive detection of disease biomarkers, viruses, and bacteria.

In addition, photonic crystals have facilitated the development of highly miniaturized biosensors that can be integrated into portable devices [16]. By manipulating the photonic crystal's properties, such as its bandgap and surface chemistry, biosensors can be designed to target a wide range of biological molecules [17]. Photonic crystal biosensors are finding immense applications in medical applications

Abdullah Al-Mamun Bulbul and al have modeled and quantitatively analyzed a hollow-core PCF to evaluate its performance as a biosensor specifically designed to sense four types of cancerous cells [18]. A.V. Orlov and developed a biosensor for the diagnostics of autoimmune diseases by highly sensitive measuring in human serum [19].



Maria Fernanda Pineda designated a biosensor based on PHc structures for the detection of viable Rotaviruses [20].

Photonic crystal biosensors have evolved with more capabilities, however, they are limited to only specific analytes and face challenges related to sensitivity. The authors' recent individual papers [21], [22], [23], [24], and [25] present innovative designs and simulations capable of efficiently detecting a variety of viruses and diseases. These simulations demonstrate remarkable evolutions in wavelength capabilities, which include sensitivities ranging from 400 nm/RIU, 546.72 nm/RIU, 650 nm/RIU, 881.25 nm/RIU to 1330 nm/RIU, respectively.

### 1. Definition

A photonic crystal is defined as a periodical dielectric structure with a frequency of refractive index of the order of the wavelength of the localized light. Since its inception, the number of publications related to PHc has been explosive. Schematic images in one, two, and three dimensions (1d, 2d and 3d) [26].

The dielectric mirror, or Bragg reflector, is a stack of alternating layers of material with periodic high and low refractive indices. The one-dimensional periodic variation of the refractive index  $n$  in figure i.2 represents one of the simplest periodic structures within a general class of optical materials called photonic crystals. A photonic crystal (PHc) is a material that has been structured to have a periodic modulation of the refractive index  $n$  so that the structure influences the propagation and confinement of light within it.

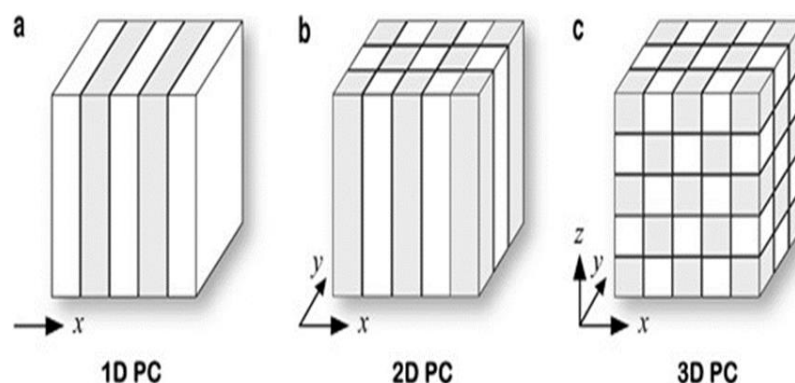


Figure 1 : Photonic crystals in (a) 1D, (b) 2D, and (c) 3D, D being the dimension [27].

Grey and white regions have different refractive indices and are not necessarily of the same size.  $\Lambda$  is the periodicity. The photonic crystal 1d in (a) is the well-known Bragg reflector, a dielectric stacking.

Periodicity can be one-dimensional (1d), two-dimensional (2d), or three-dimensional (3d); figures 1 (a) to (c) illustrate single photonic crystals 1d, 2d, and 3d as examples. Indeed, we can build rather complicated structures that have very interesting optical properties.

## 2. Basic properties of photonic crystals

### 2.1.1D Photonic Crystals (one-dimensional)

These structures are commonly known as the Bragg network. They are generally made by stacking layers of refractive index  $n_1$  and  $n_2$  respectively, the layers have an optical thickness equal to  $\lambda/4$ ,  $\lambda$  being the guided wavelength around which the material must prohibit the propagation of electromagnetic waves under normal incidence [28]. Figure 2 represents the one-dimensional periodic structure.

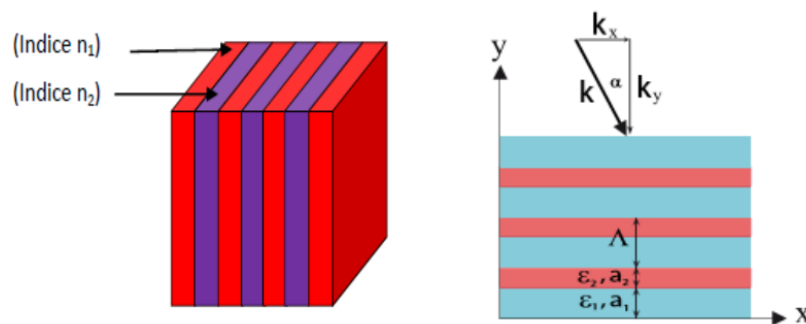


Figure 2: One-dimensional periodic structure [29].

### 2.2.3D Photonic Crystals (three-dimensional)

Three-dimensional photonic crystals are structures whose dielectric permittivity is periodically structured in all three directions. They were the second to be carried out by Yablonovich after the Bragg networks. Its objective was to obtain a complete forbidden band for all directions of space to inhibit the spontaneous emission of light [30].

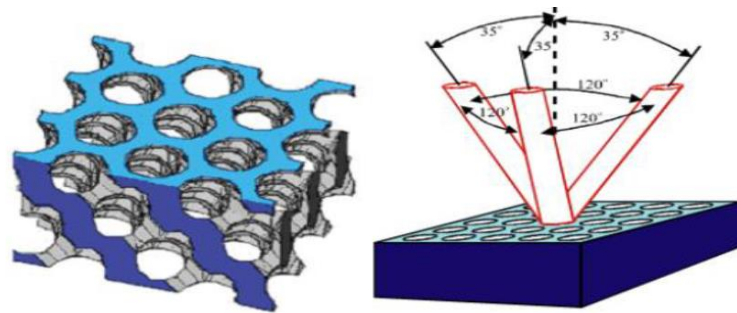


Figure 3 : The first BIP3D structure: yablonovite[1].

### 2.3.2D Photonic Crystals (two-dimensional)

A two-dimensional photonic crystal is a structure that has a periodic modulation of dielectric permittivity  $\epsilon$  in two directions in space, and is homogeneous in the third.

These periodic structures are composed of dielectric cylinders. They present a relative geometric simplicity that facilitates theoretical and experimental studies [32].

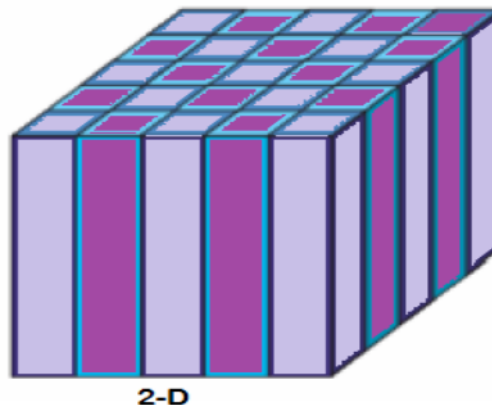


Figure 4 : Two-dimensional periodic structure [33].

There are two types of dielectric periodic structures:

- So-called “connected” structures (Fig 5): the elementary patterns are the  $n_1$  index lower than the  $n_2$  index of the dielectric matrix[2].
- So-called “disconnected” structures (Fig 5): the elementary motifs have an index of  $n_1$  higher than the index of  $n_2$  of the inter-motif space. They consist of dielectric or metallic rods periodically aligned in air or foam[2].

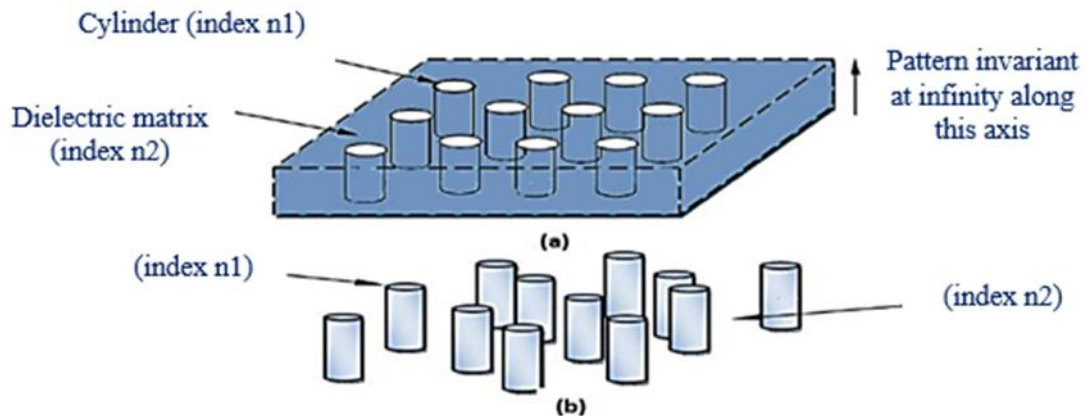


Figure 5 : (a) Connected 2D structure (b) Disconnected 2D structure [34].

To open wide forbidden bands, a contrast of  $\Delta n$  (the difference between the indices of the medium and the stems) must be sufficiently large. In two dimensions, it is necessary to consider two different polarizations: TE (with the field  $E$  perpendicular to the axis of the holes) and TM (where  $E$  is parallel to the axis of the holes). Many theorists have sought to optimize the dimensions of structures to obtain complete forbidden bands even if they have applications. There are three main families of 2D PBG materials according to the shape of the network:

- **Square mesh:**

The primitive mesh is a square on the side. Its Brillouin area is a rectangle isosceles triangle.

- **Triangular network:**

This network allows the opening of the widest forbidden bands in the plane. The network is described by direct vectors  $\vec{a}_1$  and  $\vec{a}_2$ .

- **Hexagonal Array:**

By removing some patterns from the previous array, a hexagonal array can be obtained.

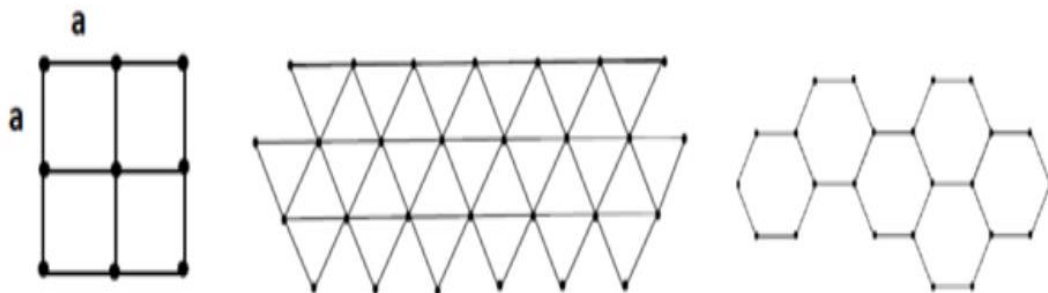


Figure 6 : Representation (a) of a square network (b) of a triangular network (c) of a hexagonal network [35].

### *Note01:*

When compared to 1DPHc and 3DPHc, the 2DPHc sensor-based attracts increased attention from the scientific community due to its comparatively simple pattern, small size, good light confinement, accuracy in band gap calculation, and ease of integration. That's why we focus our study on 2DPHc [36].

### ● **Band Diagram:**

Any photonic crystal is characterized by its band diagram. The band diagram represents the variations in frequencies allowed in the network as a function of the projection of the wave vector along the directions of high symmetry of the latter. It is represented in reduced units. If we consider the case of a triangular network of permittivity ( $\epsilon=12$ ), the band diagram is represented as follows:

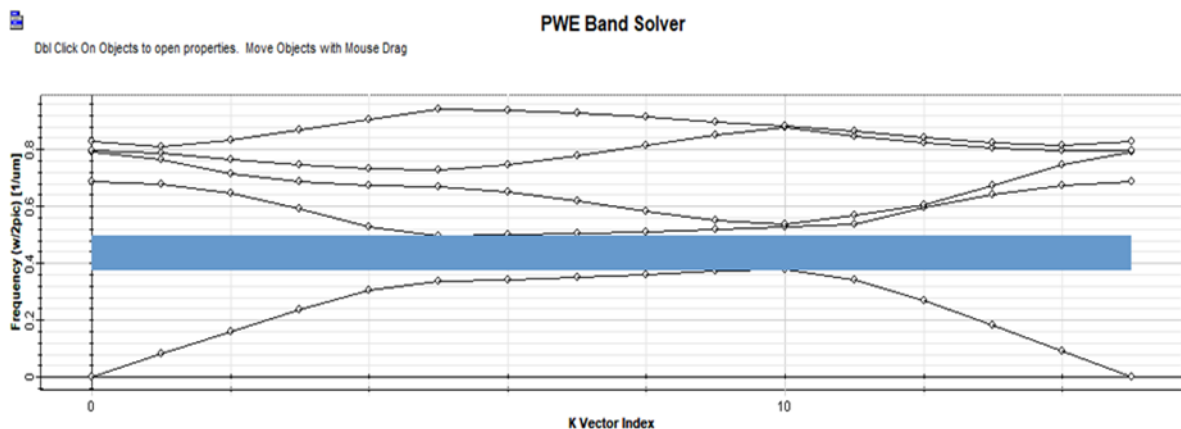


Figure 7 : Band diagram of a hexagonal two-dimensional photonic crystal. (Our works)

### **2.4. Defects in 2D photonic crystals**

Several types of defects are possible and allow certain applications, such as high selectivity filters since only the electromagnetic wave whose frequency corresponds to that of the allowed mode will be transmitted or even tunable filters. Imperfection in the periodic arrangement of the dielectric structure is a simple way to create one or more modes allowed in the gap to introduce a defect in the crystal. In the case of two-dimensional photonic crystals of particular interest to us in this work, several types of defects can be considered.

### 2.4.1. Linear defect

A guide is a linear defect introduced into a photonic crystal if it is repeated in two directions in space. The 2D photonic crystal consists of either dielectric columns surrounded by air or air holes engraved through a dielectric matrix. A waveguide can then be created by discarding two half-planes as shown in (Fig 8). The difference between the two semi-planes, the crystal direction, and the symmetry of the edges define a single guide.

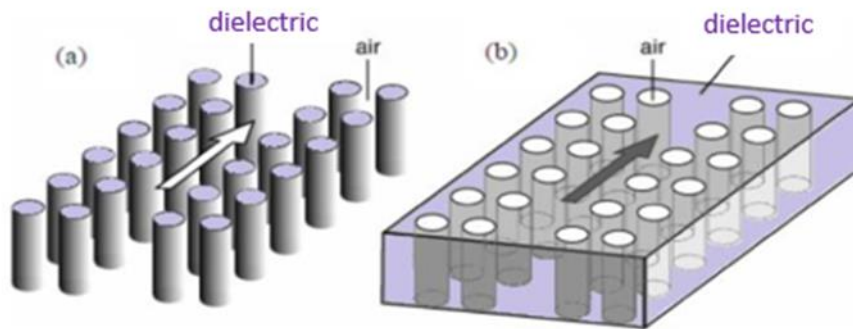


Figure 8 : Diagram of a faulty guide in a network (a) of columns of a dielectric (b) of air holes [37].

### 2.4.2. Point defects

Point defects are created by changing the characteristics of a cell in the network. To use the terminology of crystal physics, then flaws or substitution can be achieved. This corresponds to a microcavity inside the photonic crystal. Fig (9) represents the different types of defects  $\mu$ .

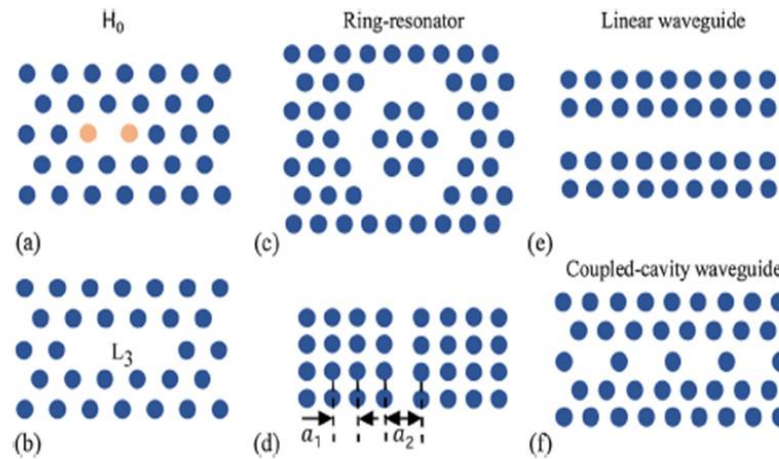


Figure 9 : Different types of defects (a)  $H_0$ -cavity. (b)  $L_3$ -cavity. (c) Ring resonator. (d) Hetro-structure cavity. (e) Linear waveguide. (f) Coupled-cavity waveguide [38].

### 3. Applications of photonic crystals

The applications of photonic crystals are multiple and affect many fields. Most of these applications are in:

- Optic[39].
- Telecommunication[40].
- Sensors[41].
- Imaging[42].
- Solar energy fields[43].

### Photonic Crystal Sensors

#### 3.1. Definition of a sensor

A sensor is a device transforming the state of an observed physical quantity into a usable quantity, such as an electric voltage, a frequency, a measurement height, an intensity, or the deviation of a needle (Fig.10). We can say that a sensor is a device which, under the effect of a physical quantity that we wish to know and characterize, delivers an exploitable physical quantity, we thus speak of a transducer. Influence quantities are external quantities that, depending on their nature and importance, can cause disturbances on the sensor. Among the main quantities of influence: temperature, pressure, humidity, and chemical concentration[44].

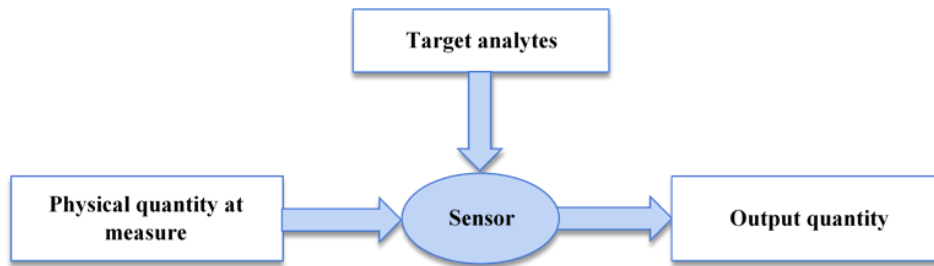


Figure 10 : Definition of a sensor[44].

The development of high-performance phc sensors is made possible by focusing on the different mechanisms of external physical interactions that we wish to characterize.

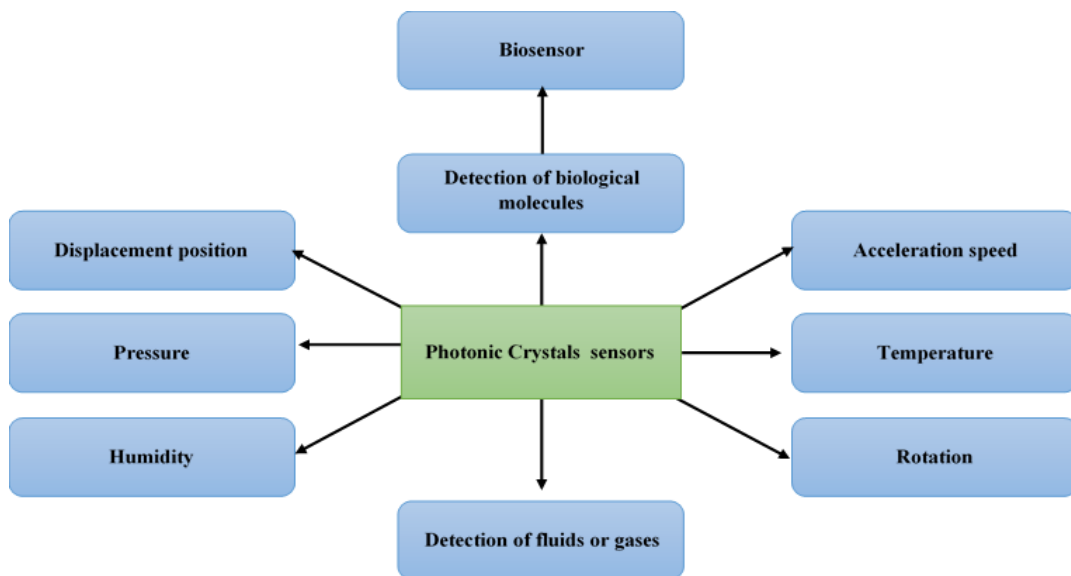


Figure 11 : Some examples of physical quantities detectable by phc means [45].

### Note 02:

Photonic crystal sensors based on refractive index detection as described below have the advantage of converting a sensor into a biosensor with the change of the analyte type .in our study we chose the RBC components and uric acid as biological analyte.

## 4. Mechanism of detections

Photonic crystals can be used for sensing applications by exploiting changes in their optical properties. Here are some of the mechanisms of detection in photonic crystals:

### 4.1.Absorption sensing



Photonic crystals can be designed to have high absorption at specific wavelengths, which can be used to detect the presence of a target molecule that absorbs light at that wavelength. This can be achieved by functionalizing the surface of the photonic crystal with a molecule that specifically binds to the target molecule [46].

### **4.2.Fluorescence sensing**

Photonic crystals can be designed to enhance fluorescence signals from fluorophores attached to their surface, which can be used to detect the presence of a target molecule that binds to the fluorophore [47].

### **4.3.Surface Plasmon resonance sensing**

Photonic crystals can be combined with metallic nanoparticles to create surface Plasmon resonance (SP sensors, which can detect changes in the refractive index of a surrounding medium by monitoring changes in the SPR wavelength Overall, the mechanisms of detection in photonic crystals depend on the specific design of the photonic crystal structure and the sensing application being targeted[48].

### **4.4.Refractive index sensing**

#### **4.4.1. Band gap variation:**

Photonic crystals can be used for refractive index sensing, which involves detecting changes in the refractive index of a surrounding medium. This can be achieved by monitoring changes in the photonic bandgap, which is the range of wavelengths that cannot propagate through the photonic crystal structure[49].

#### **4.4.2. Wavelength shift sensing:**

Changes in the refractive index of a surrounding medium can cause a shift in the photonic bandgap of a photonic crystal, which can be detected by measuring the shift in the wavelength of light reflected by the photonic crystal[50].

## **5. Characteristic paramètres**

### **5.1.Sensitivity(s)**

Two types of definitions are mostly used for photonic crystal sensors in the literature. For some structures the intensity of trans-mission changes when an analyte is introduced.

Another sensitivity definition is used for sensors that experience a resonance wavelength shift for different refractive indexes.

$$s = \frac{\Delta\lambda}{\Delta n} \quad (\text{I. 1})$$

Where  $\Delta\lambda$  is the resonant wavelength shifting by considering the cavity without the liquid infiltrated and  $\Delta n$  is the alteration in the RI due to the liquid analyte that infiltrated the cavity[51].

### 5.2.The detection limit

The detection limit is the minimal physical change that can be detected. It can be calculated by:

$$LD = \frac{FWHM}{s} \quad (\text{I. 2})$$

(FWHM full-width half maximum, S the sensitivity)[52].

### 5.3.Quality factor

The quality factor which is defined as the ratio of the resonance wavelength to the bandwidth measured at full-width half maximum (FWHM) is a parameter that models the field confinement in a cavity [52]. To have a higher sensitivity, the quality factor needs to be as high as possible. Defines the quality factor:

$$Q = \frac{\lambda(\text{resonance})}{\Delta\lambda(\text{FWHM})}. \quad (\text{I. 3})$$

### 5.4.Figure of merit

To compare the performance of biosensors, having a well-defined figure of merit (FoM) is the key parameter[53]. It is usually defined by dividing the sensitivity of the biosensor by its FWHM bandwidth:

$$F_oM = \frac{S}{\Delta\lambda(FWHM)} [RIU^{-1}]. \quad (I. 4)$$

### 6. Objective

This work aims to improve the sensitivity of a two-dimensional photonic crystal biosensor used for chikungunya virus detection. Where the optiFDTD of the OPTIWAVE package and the PWE was used as software simulators.

### Conclusion:

PHc have a wide range of applications in many optical systems, Refractive index measurement is one of the many methods used for the diagnosis of chikungunya virus, The sensitivity of many PHc cavities is usually high enough to sense small changes in refractive indices which can be induced due to concentration changes of the analyte in order of 0.01 of refractive index unit (RIU). In this work, we have tried to provide higher sensitivity to refractive index variations. The OptiFDTD of OPTIWAVE and the PWE were used.

## Bibliographic references

- [1] Y. Merle, ‘Study of electromagnetic dispersion in two-dimensional dielectric materials’, Doctoral theses, Limoges, 2003. Accessed: May 30, 2023. [Online]. Available: <https://www.theses.fr/2003LIMO0045>
- [2] H. Oualid, M. Khaled, and O. Hamza, ‘Study and Simulation of Electromagnetic Wave Propagation in Photonic Crystal Guides’, Jul. 2018, Accessed: May 31, 2023. [Online]. Available: <http://dspace.univ-ouargla.dz/jspui/handle/123456789/18719>
- [3] L. P. Biró *et al.*, ‘Role of photonic-crystal-type structures in the thermal regulation of a Lycaenid butterfly sister species pair’, *Phys. Rev. E*, vol. 67, no. 2, p. 021907, Feb. 2003, doi: 10.1103/PhysRevE.67.021907.
- [4] Yablonovitch, E; Gmitter, T; Leung, K (1991). "Photonic band structure: The face-centered-cubic case employing nonspherical atoms". *Physical Review Letters*. 67 (17): 2295–2298. Bibcode:1991PhR
- [5] V. N. Astratov *et al.*, ‘Optical spectroscopy of opal matrices with CdS embedded in its pores: Quantum confinement and photonic band gap effects’, *Il Nuovo Cimento D*, vol. 17, no. 11, pp. 1349–1354, Nov. 1995, doi :10.1007/BF02457208.
- [6] T. F. Krauss, R. M. D. L. Rue, and S. Brand, ‘Two-dimensional photonic-bandgap structures operating at near-infrared wavelengths’, *Nature*, vol. 383, no. 6602, Art. no. 6602, Oct. 1996, doi: 10.1038/383699a0.
- [7] V. Saranathan, S. Narayanan, A. Sandy, E. R. Dufresne, and R. O. Prum, ‘Evolution of single gyroid photonic crystals in bird feathers’, *Proc. Natl. Acad. Sci.*, vol. 118, no. 23, p. e2101357118, Jun. 2021, doi: 10.1073/pnas.2101357118.
- [8] ‘en.fr.edu.vn | 522: Connection timed out’. [https://en.fr.edu.vn/en/Photonic\\_crystal](https://en.fr.edu.vn/en/Photonic_crystal) (accessed Jun. 01, 2023).
- [9] J. W. Galusha, L. R. Richey, J. S. Gardner, J. N. Cha, and M. H. Bartl, ‘Discovery of a diamond-based photonic crystal structure in beetle scales’, *Phys. Rev. E*, vol. 77, no. 5, p. 050904, May 2008, doi: 10.1103/PhysRevE.77.050904.

- [10] ‘Brilliant camouflage: photonic crystals in the diamond weevil, *Entimus imperialis* | Proceedings of the Royal Society B: Biological Sciences’.  
<https://royalsocietypublishing.org/doi/abs/10.1098/rspb.2011.2651> (accessed Jun. 01, 2023).
- [11] B. D. Wilts, K. Michielsen, H. De Raedt, and D. G. Stavenga, ‘Hemispherical Brillouin zone imaging of a diamond-type biological photonic crystal’, *J. R. Soc. Interface*, vol. 9, no. 72, pp. 1609–1614, Dec. 2011, doi: 10.1098/rsif.2011.070.
- [12] B. D. Wilts, K. Michielsen, H. De Raedt, and D. G. Stavenga, ‘Iridescence and spectral filtering of the gyroid-type photonic crystals in *Parides sesostris* wing scales’, *Interface Focus*, vol. 2, no. 5, pp. 681–687, Dec. 2011, doi: 10.1098/rsfs.2011.0082.
- [13] Y. Zhao, X. Zhao, and Z. Gu, ‘Photonic Crystals in Bioassays’, *Adv. Funct. Mater.*, vol. 20, no. 18, pp. 2970–2988, 2010, doi: 10.1002/adfm.201000098.
- [14] F. Parandin, F. Heidari, Z. Rahimi, and S. Olyaei, ‘Two-Dimensional photonic crystal Biosensors: A review’, *Opt. Laser Technol.*, vol. 144, p. 107397, Dec. 2021, doi: 10.1016/j.optlastec.2021.107397.
- [15] R. Arunkumar, T. Suaganya, and S. Robinson, ‘Design and Analysis of 2D Photonic Crystal Based Biosensor to Detect Different Blood Components’, *Photonic Sens.*, vol. 9, no. 1, pp. 69–77, Mar. 2019, doi: 10.1007/s13320-018-0479-8.
- [16] S. Robinson and N. Dhanlaxmi, ‘Photonic crystal based biosensor for the detection of glucose concentration in urine’, *Photonic Sens.*, vol. 7, no. 1, pp. 11–19, Mar. 2017, doi: 10.1007/s13320-016-0347-3.
- [17] C. Fenzl, T. Hirsch, and O. S. Wolfbeis, ‘Photonic Crystals for Chemical Sensing and Biosensing’, *Angew. Chem. Int. Ed.*, vol. 53, no. 13, pp. 3318–3335, 2014, doi: 10.1002/anie.201307828.
- [18] A. A.-M. Bulbul, H. Rahaman, and E. Podder, ‘Design and quantitative analysis of low loss and extremely sensitive PCF-based biosensor for cancerous cell detection’, *Opt. Quantum Electron.*, vol. 54, no. 2, p. 123, Jan. 2022, doi: 10.1007/s11082-022-03513-1.

- [19] A. V. Orlov *et al.*, ‘Multiplex label-free biosensor for detection of autoantibodies in human serum: Tool for new kinetics-based diagnostics of autoimmune diseases’, *Biosens. Bioelectron.*, vol. 159, p. 112187, Jul. 2020, doi: 10.1016/j.bios.2020.112187.
- [20] M. F. Pineda, L. L.-Y. Chan, T. Kuhlenschmidt, C. J. Choi, M. Kuhlenschmidt, and B. T. Cunningham, ‘Rapid Specific and Label-Free Detection of Porcine Rotavirus Using Photonic Crystal Biosensors’, *IEEE Sens. J.*, vol. 9, no. 4, pp. 470–477, Apr. 2009, doi: 10.1109/JSEN.2009.2014427.
- [21] P. R. Yashaswini, H. N. Gayathri, and P. C. Srikanth, ‘Performance analysis of photonic crystal based biosensor for the detection of bio-molecules in urine and blood’, *Mater. Today Proc.*, vol. 80, pp. 2247–2254, Jan. 2023, doi: 10.1016/j.matpr.2021.06.192.
- [22] M. Maache, Y. Fazea, I. Bile Hassan, A. A. Alkahtani, and I. Ud Din, ‘High-Sensitivity Capsule-Shaped Sensor Based on 2D Photonic Crystals’, *Symmetry*, vol. 12, no. 9, Art. no. 9, Sep. 2020, doi: 10.3390/sym12091480.
- [23] K. Chakrabarti, M. S. Obaidat, S. Mostufa, and A. K. Paul, ‘Design and analysis of a multi-core whispering gallery mode bio-sensor for detecting cancer cells and diabetes tear cells’, *OSA Contin.*, vol. 4, no. 8, pp. 2294–2307, Aug. 2021, doi: 10.1364/OSAC.431883.
- [24] A. Sahoo and A. D. Varshney, ‘Detection of viral and bacterial diseases using 2D photonic crystal-based elliptical ring resonator sensor’, *J. Nanophotonics*, vol. 17, no. 2, p. 026004, Apr. 2023, doi: 10.1117/1.JNP.17.026004.
- [25] N. A. Mohammed, O. E. Khedr, E.-S. M. El-Rabaie, and A. A. M. Khalaf, ‘Brain tumors biomedical sensor with high-quality factor and ultra-compact size based on nanocavity 2D photonic crystal’, *Alex. Eng. J.*, vol. 64, pp. 527–540, Feb. 2023, doi: 10.1016/j.aej.2022.09.020.
- [26] E. Yablonovitch, ‘Inhibited Spontaneous Emission in Solid-State Physics and Electronics’, *Phys. Rev. Lett.*, vol. 58, no. 20, pp. 2059–2062, May 1987, doi: 10.1103/PhysRevLett.58.2059.
- [27] Furumi, S. Self-assembled organic and polymer photonic crystals for laser applications. *Polym J* 45, 579–593 (2013). <https://doi.org/10.1038/pj.2012.181>.

- [28] M. S. Telli, ‘Matériaux à bandes interdites Photoniques bidimensionnels : Application au domaine des capteurs’, Thesis, Université Kasdi Merbah Ouargla, 2020. Accessed: Jun. 01, 2023. [Online]. Available: <http://dspace.univ-ouargla.dz/jspui/handle/123456789/29054>
- [29] L. Han, ‘1D Photonic Crystals: Principles and Applications in Silicon Photonics’, in *Theoretical Foundations and Application of Photonic Crystals*, IntechOpen, 2017. doi: 10.5772/intechopen.71753.
- [30] T. Tajiri, S. Takahashi, C. Harteveld, Y. Arakawa, S. Iwamoto, and W. Vos, ‘Reflectivity of three-dimensional GaAs photonic band-gap crystals of finite thickness’, *Phys. Rev. B*, vol. 101, Jun. 2020, doi: 10.1103/PhysRevB.101.235303.
- [31] Lixin Fu, Mi Lin, Zixian Liang, Qiong Wang, Yaoxian Zheng, Zhengbiao Ouyang, The Transmission Properties of One-Dimensional Photonic Crystals with Gradient Materials, *Materials*, 10.3390/ma15228049, 15, 22, (8049), (2022)..
- [32] Couture, S. Two-dimensional periodic structures of metallic wires: characterization and applications [Master's thesis, École Polytechnique de Montréal]. PolyPublish. (2011) <https://publications.polymtl.ca/610/>.
- [33] D. G. Popescu, P. Sterian, R. Bercia, and C. Bostan, ‘Second harmonic generation in photonic crystals: numerical simulation’. *Journal of Optoelectronics and Advanced Materials*. 2012
- [34] B. Leila, B. Hadjira, A. Mehadji, and L. Farah, ‘Filtre bi-bandes sélectifs en cristaux photoniques 2D pour les systèmes très hauts débits’. Master thesis. Univ Tlemcen. 27 /06 /2018
- [35] H. Lee, G. Li, and H. Monien, ‘Hubbard model on the triangular lattice using dynamical cluster approximation and dual fermion methods’, *Phys. Rev. B*, vol. 78, no. 20, p. 205117, Nov. 2008, doi: 10.1103/PhysRevB.78.205117.
- [36] Vijaya Shanthi, K., Robinson, S. Two-dimensional photonic crystal based sensor for pressure sensing. *Photonic Sens* 4, 248–253 (2014). <https://doi.org/10.1007/s13320-014-0198-8>.

- [37] S. G. Johnson, S. Fan, P. R. Villeneuve, J. D. Joannopoulos, and L. A. Kolodziejski, ‘Guided modes in photonic crystal slabs’, *Phys. Rev. B*, vol. 60, no. 8, pp. 5751–5758, Aug. 1999, doi: 10.1103/PhysRevB.60.5751.
- [38] F. Rahman-Zadeh, M. Danaie, and H. Kaatuzian, ‘Design of a highly sensitive photonic crystal refractive index sensor incorporating ring-shaped GaAs cavity’, *Opto-Electron. Rev.*, vol. 27, no. 4, pp. 369–377, Dec. 2019, doi: 10.1016/j.opelre.2019.11.007.
- [39] G. M. Burrow and T. K. Gaylord, ‘Multi-Beam Interference Advances and Applications: Nano-Electronics, Photonic Crystals, Metamaterials, Subwavelength Structures, Optical Trapping, and Biomedical Structures’, *Micromachines*, vol. 2, no. 2, Art. no. 2, Jun. 2011, doi: 10.3390/mi2020221.
- [40] M. Deubel, G. von Freymann, M. Wegener, S. Pereira, K. Busch, and C. M. Soukoulis, ‘Direct laser writing of three-dimensional photonic-crystal templates for telecommunications’, *Nat. Mater.*, vol. 3, no. 7, Art. no. 7, Jul. 2004, doi: 10.1038/nmat1155.
- [41] Q. Qiao, J. Xia, C. Lee, and G. Zhou, ‘Applications of Photonic Crystal Nanobeam Cavities for Sensing’, *Micromachines*, vol. 9, no. 11, Art. no. 11, Nov. 2018, doi: 10.3390/mi9110541.
- [42] G. Pitruzzello and T. F. Krauss, ‘Photonic crystal resonances for sensing and imaging’, *J. Opt.*, vol. 20, no. 7, p. 073004, Jun. 2018, doi: 10.1088/2040-8986/aac75b.
- [43] X. Zheng and L. Zhang, ‘Photonic nanostructures for solar energy conversion’, *Energy Environ. Sci.*, vol. 9, no. 8, pp. 2511–2532, Aug. 2016, doi: 10.1039/C6EE01182A.
- [44] E. C. Alocilja and S. M. Radke, ‘Market analysis of biosensors for food safety’, *Biosens. Bioelectron.*, vol. 18, no. 5, pp. 841–846, May 2003, doi: 10.1016/S0956-5663(03)00009-5.
- [45] A. A. Ensafi, M. Taei, H. R. Rahmani, and T. Khayamian, ‘Sensitive DNA impedance biosensor for detection of cancer, chronic lymphocytic leukemia, based on gold nanoparticles/gold modified electrode’, *Electrochimica Acta*, vol. 56, no. 24, pp. 8176–8183, Oct. 2011, doi: 10.1016/j.electacta.2011.05.124.



- [46] X. Yu, Y. Sun, G. B. Ren, P. Shum, N. Q. Ngo, and Y. C. Kwok, ‘Evanescent Field Absorption Sensor Using a Pure-Silica Defected-Core Photonic Crystal Fiber’, *IEEE Photonics Technol. Lett.*, vol. 20, no. 5, pp. 336–338, Mar. 2008, doi: 10.1109/LPT.2007.915659.
- [47] S. Smolka, M. Barth, and O. Benson, ‘Highly efficient fluorescence sensing with hollow core photonic crystal fibers’, *Opt. Express*, vol. 15, no. 20, pp. 12783–12791, Oct. 2007, doi: 10.1364/OE.15.012783.
- [48] C. Liu *and al.*, ‘Symmetrical dual D-shape photonic crystal fibers for surface plasmon resonance sensing’, *Opt. Express*, vol. 26, no. 7, pp. 9039–9049, Apr. 2018, doi: 10.1364/OE.26.009039.
- [49] ‘Multiplication of photonic band gaps in one-dimensional photonic crystals by using hyperbolic metamaterial in IR range | Scientific Reports’.  
<https://www.nature.com/articles/s41598-023-27550-2> (accessed Jun. 01, 2023).
- [50] T. Li, G. Liu, H. Kong, G. Yang, G. Wei, and X. Zhou, ‘Recent advances in photonic crystal-based sensors’, *Coord. Chem. Rev.*, vol. 475, p. 214909, Jan. 2023, doi: 10.1016/j.ccr.2022.214909.
- [51] I. M. White and X. Fan, ‘On the performance quantification of resonant refractive index sensors’, *Opt. Express*, vol. 16, no. 2, pp. 1020–1028, Jan. 2008, doi: 10.1364/OE.16.001020.
- [52] T. Christopoulos, O. Tsilipakos, G. Sinatkas, and E. E. Kriezis, ‘On the calculation of the quality factor in contemporary photonic resonant structures’, *Opt. Express*, vol. 27, no. 10, pp. 14505–14522, May 2019, doi: 10.1364/OE.27.014505.
- [53] S. Chen and C. Lin, ‘Figure of merit analysis of graphene-based surface plasmon resonance biosensor for visible and near infrared’, *Opt. Commun.*, vol. 435, pp. 102–107, Mar. 2019, doi: 10.1016/j.optcom.2018.11.031.

# **Chapter 02**

Software and the simulation method

### **Introduction**

OptiFDTD is a powerful, highly integrated, and easy-to-use software that enables computer-aided design and simulation of advanced passive photonic components. The OptiFDTD software package is based on the Finite Difference Time Domain (FDTD) method. The FDTD method has become a powerful engineering tool for simulating integrated and diffractive optics. This is due to a unique combination of features such as the ability to simulate light propagation, scattering, and diffraction, as well as reflection and polarization effects. It also simulates material anisotropy and dispersion without pre-assuming field behavior, such as slowly varying amplitude approximations. This method enables efficient and powerful simulation and analysis of submicron devices with very fine structural details. The submicron scale implies a high degree of light confinement, and as a result, the refractive indices of materials (mainly semiconductors) used in typical device designs vary widely[1].

This chapter aims to highlight the potential of photonic crystals and the simulation methods used for the photonic crystals on which the simulation software (FDTD and PWE) is based.

### **1. Modulation Methods and software**

The most commonly cited methods in the literature to study photonic crystals, and the ones we use in our OptiFDTD software simulations, are the plane wave method (PWE) and the finite difference in time method (FDTD).

#### **1.1. The FDTD method**

The FDTD method is one of the most widely used methods in electromagnetics. The first algorithm was proposed by Yee in 1966. This approach is particularly useful for understanding the spectral response of systems that are not necessarily periodic and for computing field distributions of infinite-dimensional structures. FDTD can not only calculate the energy band diagram but also simulate the time evolution of the electromagnetic field in photonic crystals, which makes it possible to obtain information on many other quantities such as the Poynting vector or electromagnetic energy. Storage. It includes the space and time point derivatives that appear in Maxwell's equations by central finite difference approximations.

### **1.2.The PWE method**

The plane wave decomposition method is a method for solving Maxwell's equations in the frequency domain. It is based on decomposing electromagnetic problems into plane waves. This method is mainly used to analyze the dispersion properties of materials with photonic bandgap and can determine the frequency, polarization, symmetry, and field distribution of photonic structural modes[2].

## **2. OptiFDTD**

OptiFDTD is a powerful, highly integrated, and easy-to-use software application that enables computer-aided design and simulation of advanced passive and nonlinear photonic components.

Using OptiFDTD, you can design, analyze and test advanced passive and nonlinear photonic components for wave propagation, scattering, reflection, diffraction, polarization, and nonlinear phenomena. The core of OptiFDTD is based on the second-order numerical precision finite-difference time-domain (FDTD) algorithm and the most advanced constraints - uniaxial perfectly matched layer (UPML) constraints. The algorithm solves for the electric and magnetic fields in the time and space domains using the full vector differential form of Maxwell's coupled Curl equations. This means that any model geometry is possible and there are no restrictions on the material properties of the device.

Automating these processes greatly increases designer productivity and reduces time to market. This integration with other Optiwave software for photonic design automation contributes to faster return on investment and shorter payback periods.

### **2.1.Specific Benefits**

- Presents a global overview of photonics problems.
- Provides broad material choice.
- Offers extensive excitation selection.
- Delivers powerful Post-Data Processing.

## 2.2.Applications

OptiFDTD enables the simulation of:

- Photonic band gap materials and devices.
- Optical micro-ring filters and resonators.
- Grating-based waveguide structures.
- Diffractive micro-optic elements.
- Complex integrated optics structures.
- Nonlinear materials, dispersive materials, surface plasma, and anisotropic materials.
- Photonic surface plasmon and surface plasma wave.
- Nano-particles, cells, tissue, and lens.
- Electromagnetic phenomena[3].

## 2.3.OptiFDTD coordinates system

OptiFDTD uses a different coordinate system than most 3D layout and editing programs. The coordinate system is defined to be compatible with other Optiwave software such as OptiBPM. The representation of the coordinate system used is shown below.

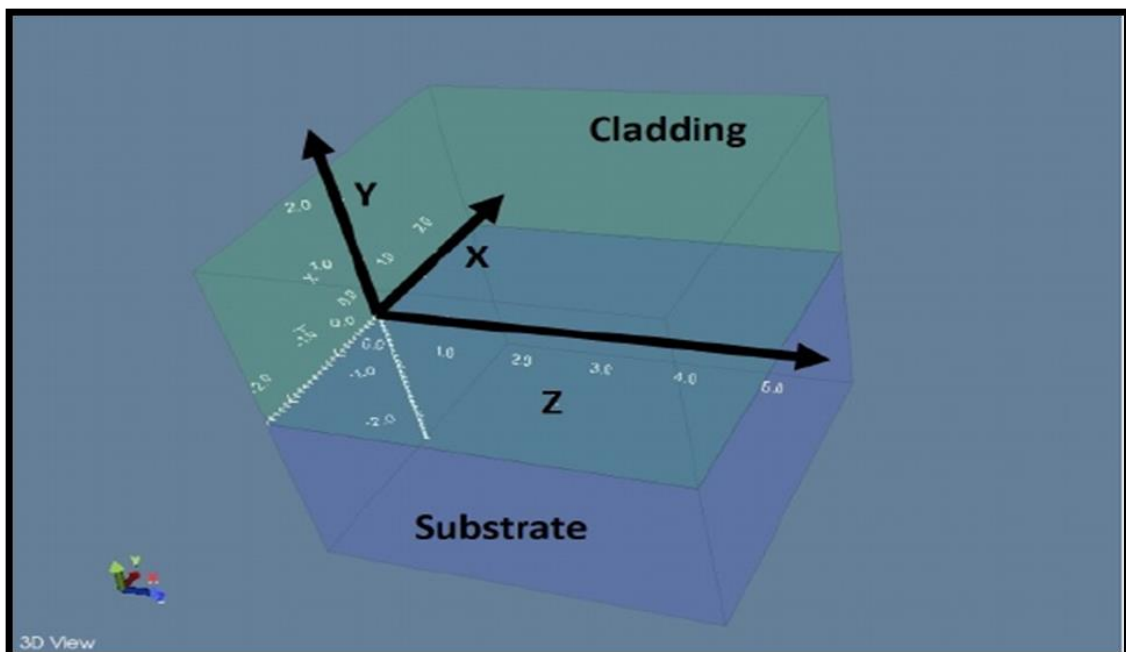


Figure 12 : The coordinate system used in OptiFDTD.

The regions named are used to separate volumes below and Substrate Cladding above the XZ ( $Y=0$ ) plane. They are used to represent traditional waveguides fabricated using lithography for example. Substrate and Cladding regions can have different background materials attached to them. While working with OptiFDTD, you must take note of the following conventions:

- X is referred to as the width or vertical component
- Y is referred to as the depth
- Z is referred to as the length or horizontal component
- The 2D and 3D simulation domains are referred to as 2D and 3D wafers.

It is possible to run either 2D or 3D simulations using OptiFDTD. In the case of 2D simulations, the simulation region is defined by the XZ plane[4].

### **3. Work on the program (optiFDTD)**

Use the OptiFDTD Designer program to create simulation objects and define their properties. We define some basic geometry and run simulations and verify results based on how we identify sources and detectors. OptiFDTD Designer is one of the four components of OptiFDTD.

Creating and running FDTD simulations with OptiFDTD can be done using four main programs, as described below:

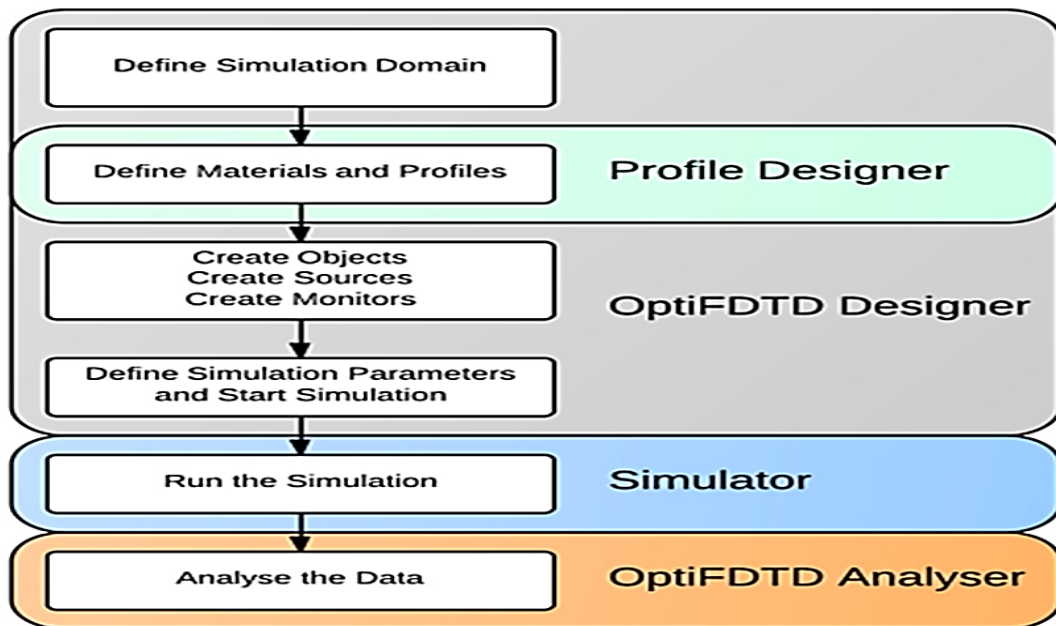


Figure 13 : The workflow of a typical simulation using OptiFDTD.

### 3.1.OptiFDTD Designer

The main OptiFDTD program. From here, you can create new designs, set simulation parameters, write scripts and start simulations. Data are saved in a project file with the extension. fdt.

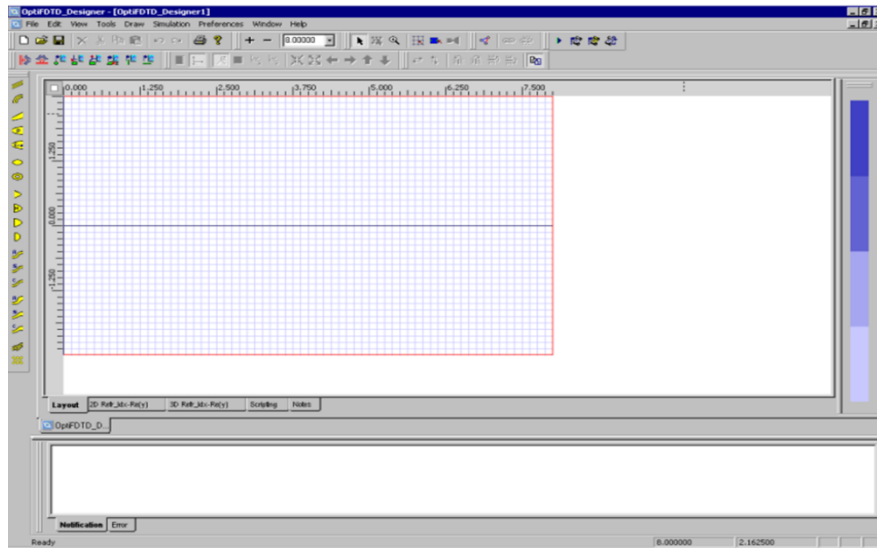


Figure 14 : OptiFDTD Designer window.

Layout Designer – This is where you define your structure and draw the design, set simulation parameters, write scripts and start simulations. Data are saved in a project file with the extension. fdt. Crystal lattice properties appear in the following window:

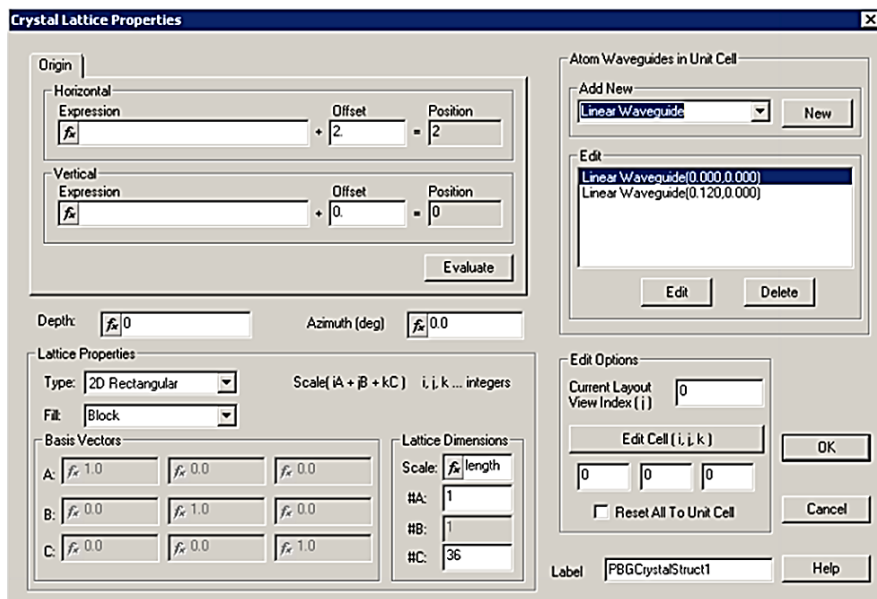


Figure 15 : Crystal lattice properties (setting of structure).



### 3.2.Profile Designer

This program is used to define all the materials and profiles used in the simulation region.

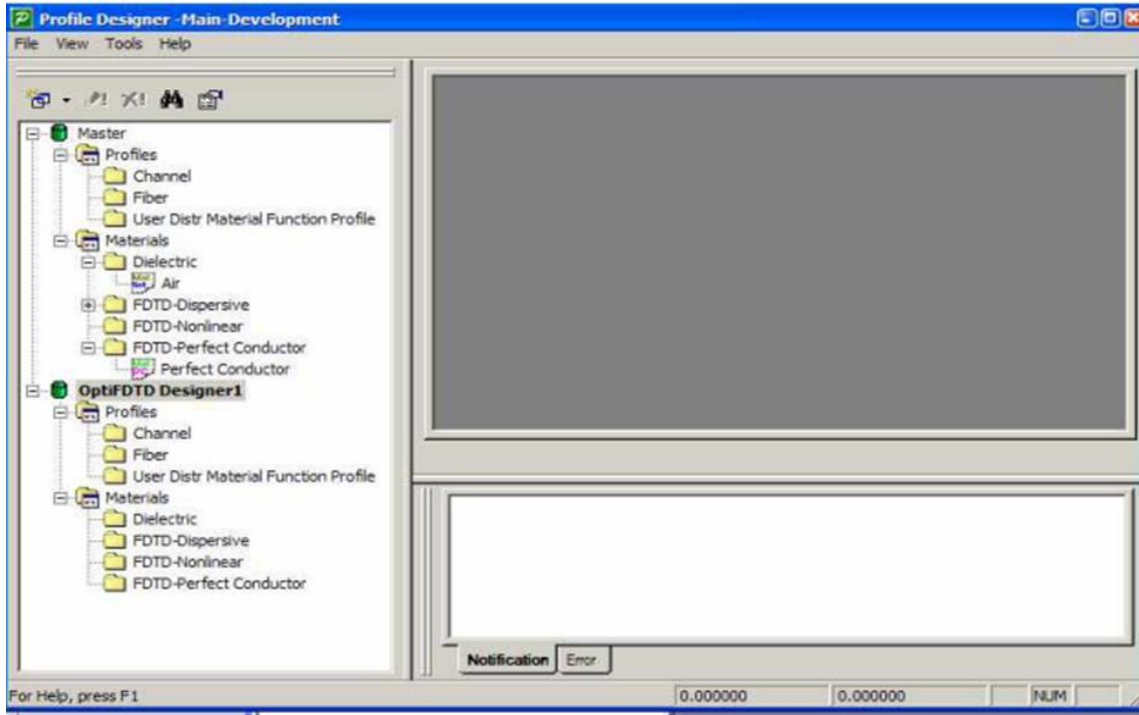


Figure 16: Profile designer (materials and profile used).

Profiles are a special type of object used to define cross-sections of waveguides. As following:

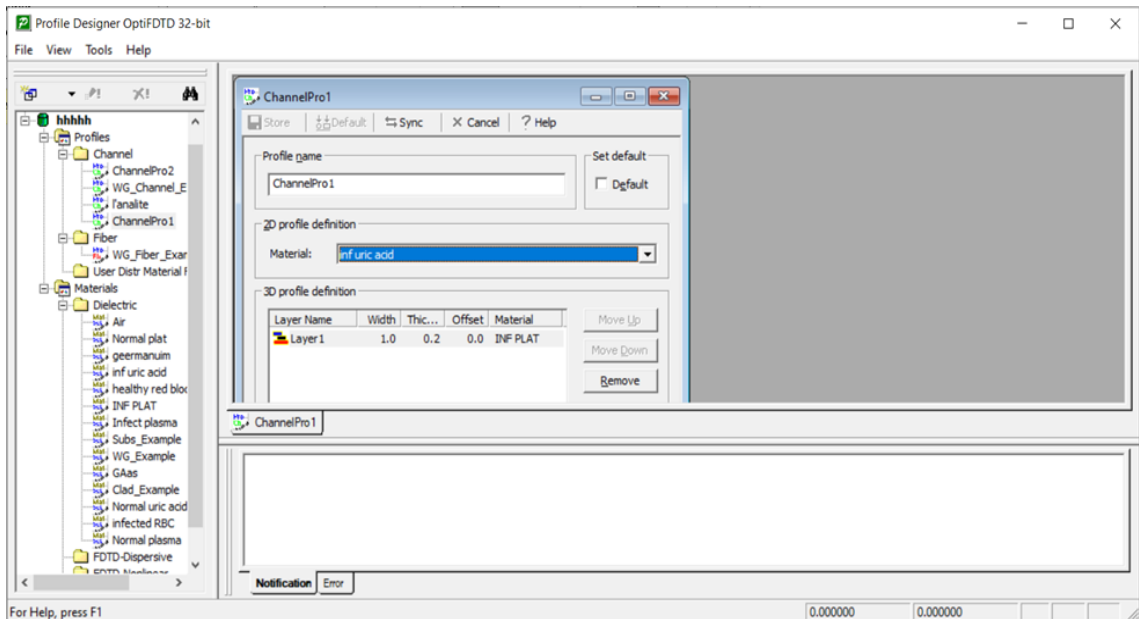


Figure 17 : profile definition window.

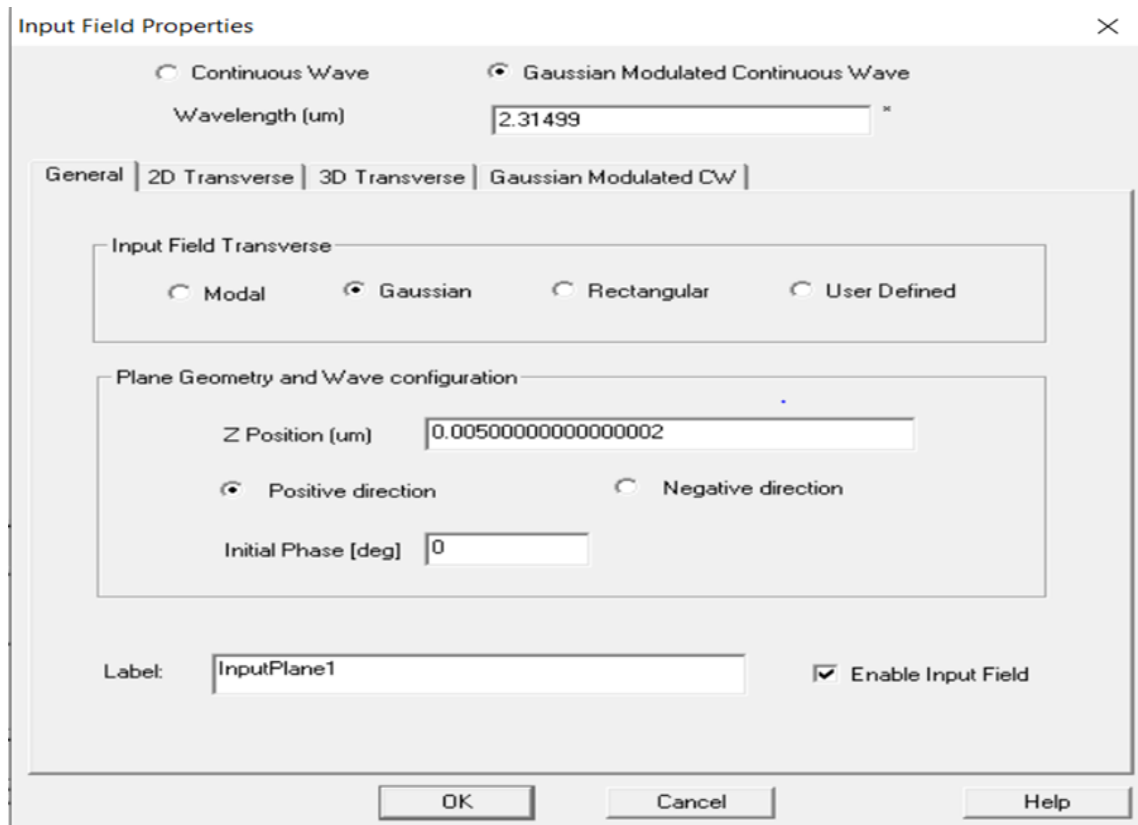


Figure 18 : Input field properties.

### 3.3. OptiFDTD Simulator

Processes project files designed in OptiFDTD\_Designer (.fdt).

OptiFDTD\_Simulator opens automatically when you start a simulation. The simulation results are stored in a file with the extension. fda.

Contains extensive viewing options and analysis features, and has the facility to export data to other file formats. A typical FDTD simulation design sequence can be defined as this:

first, define the simulation domain sizes, then define materials and profiles to be used in the simulation, then create the objects, light sources, and detectors that compose the simulation, run the simulation, and finally analyze the results. The workflow of a typical simulation using OptiFDTD is shown below.

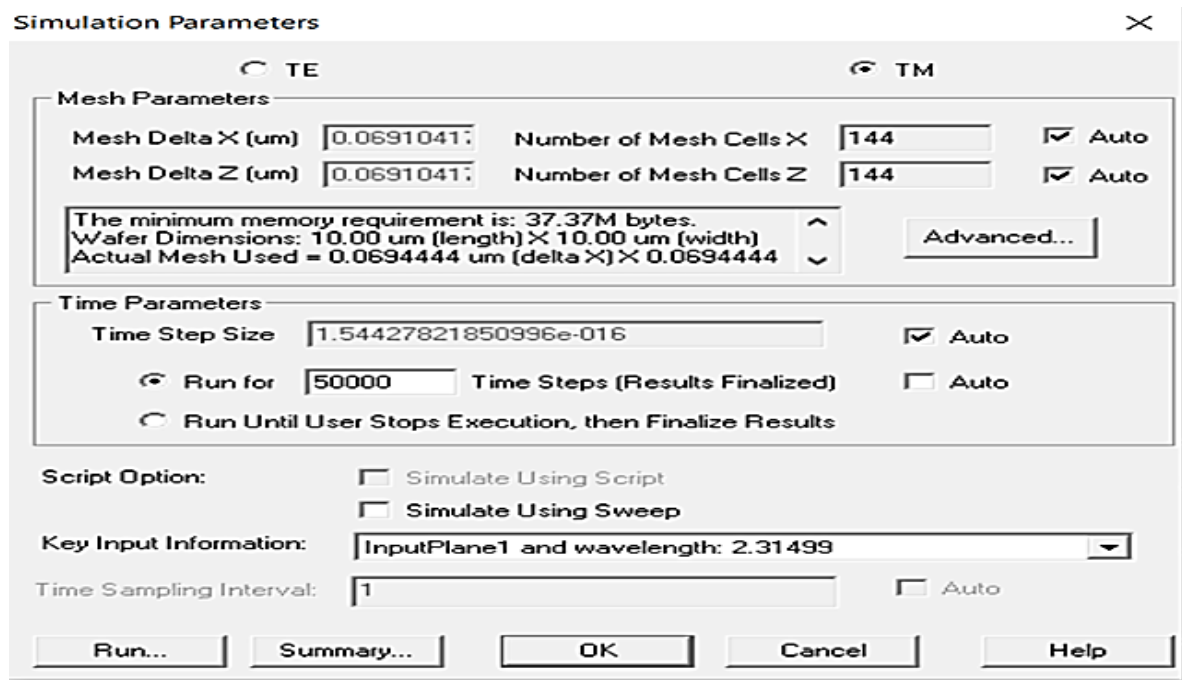


Figure 19 : Setting of simulation.

You can choose to open OptiFDTD\_Analyzer at the end of the simulation. Loads and analyzes the result files produced by OptiFDTD Simulator (.fda).

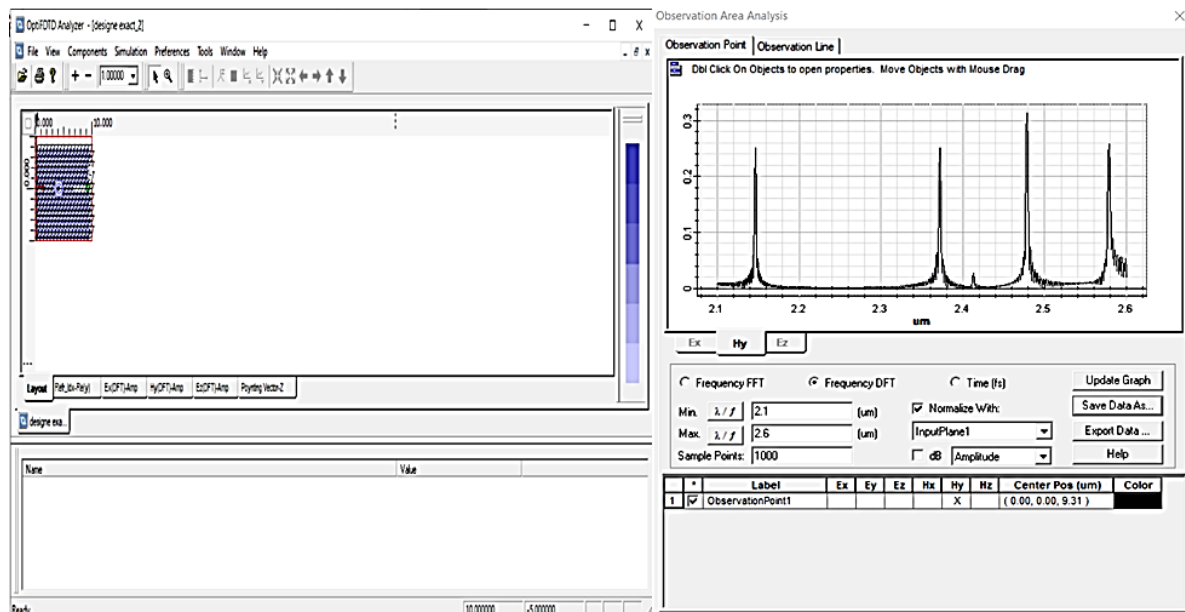


Figure 20 : OptiFDTD analyze and observation Area Analysis.

At the same time, we can even see the superposition of more than one or two peaks with more properties (color.....)

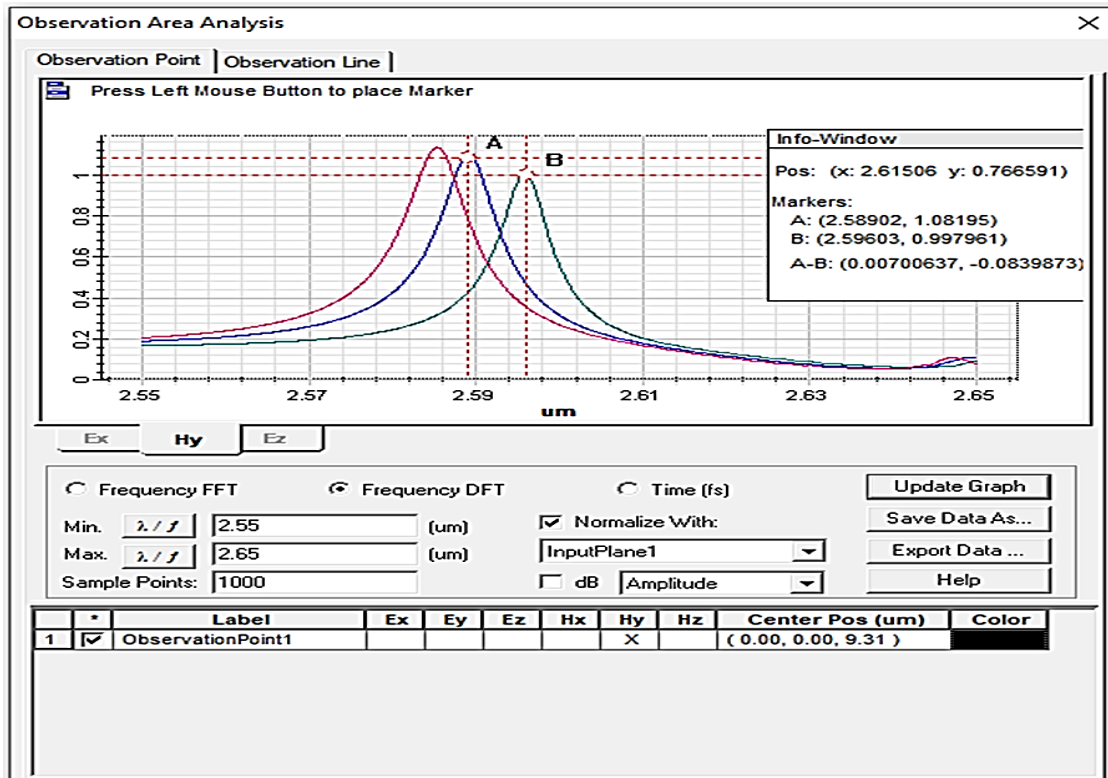


Figure 21 : Observation results and superposition curves (in colors).

Here, you can see the final result of your simulation like the final taps (stage).

## Conclusion

In this chapter, the optiFDTD software and the modulation methods such as the FDTD and the PWE methods worked on have been presented in addition to a brief tutorial software.

In the following chapter, we will present the design of the 2D photonic crystal-based biosensor simulated by optiFDTD for chikungunya virus detection, where results of the photonic band diagram and the transmission response will be discussed.

## **Bibliographic references**

- [1] S. Ge, 'OptiFDTD Publication References *Optiwave*, <https://optiwave.com/resources/publications/optifdtd-publication-references-2020/> (accessed Jun. 02, 2023).
- [2] K. S. Yee, 'Numerical solution of initial boundary value problems involving Maxwell's equations in isotropic media', *IEEE Trans Antennas Propag.*, vol. 14, pp. 302–307, 1966.
- [3] 'HRU Innovation beyond perfection'. <https://www.hrunisys.com/> (accessed Jun. 02, 2023).
- [4] S. Ge, 'Optiwave Invites you to ECIO 2023', *Optiwave*, Apr. 13, 2023. <https://optiwave.com/resources/upcoming-events/optiwave-invites-you-to-ecio-2023/> (accessed Jun. 02, 2023).

# **Chapter 03**

**High Sensitivity Refractive Index Sensor based on a  
photonic crystal for the detection of Chikungunya  
virus**

## Introduction

Chikungunya virus disease is a mosquito-borne viral disease that primarily affects the joints, causing severe joint pain and swelling. It also causes fever, headache, muscle pain, and rash [1]. The name "chikungunya" is derived from the Makonde language, spoken in Tanzania and Mozambique, and means "to become contorted," which describes the posture of people affected by the disease. The virus was first isolated in Tanzania in 1952, but cases have been reported in Africa, Asia, Europe, and the Americas. The virus is transmitted by mosquitoes of the *Aedes* genus, particularly *Aedes aegypti* and *Aedes albopictus*, which are also responsible for the transmission of dengue fever and Zika virus [2].

People at risk for more severe disease include newborns infected around the time of birth, older adults (more than 65  $\geq$  years), and people with medical conditions such as high blood pressure, diabetes, or heart disease [3].

Chikungunya virus is known to target red blood cells whose refractive index is 1.40, causing them to become deformed and leading to a reduction in the number of red blood cells in the body becomes its refractive index is 1.39 [4]. This can lead to anemia and other complications [5]. The virus can also affect platelets, which are responsible for blood clotting a condition known as thrombocytopenia where their refractive index converts from 1.35 to 1.33, this can cause bleeding, bruising, and other complications, particularly in vulnerable populations such as pregnant women mostly during the second trimester and the elderly. Intrapartum transmission has also been documented when the mother was viremic around the time of delivery [6].

Research has also suggested that the chikungunya virus can affect the immune system, causing it to produce certain antibodies that can lead to further complications. For example, some studies have suggested that the virus can trigger the production of autoantibodies, which can cause damage to healthy cells and tissues in the body [7]. Early detection of chikungunya virus disease is crucial for the effective management of the disease. Biomedical research has focused on developing diagnostic tools that can detect the virus quickly and accurately [8].

The detection of the Chikungunya virus in a biosensor involves the use of specific antibodies that can bind to the virus and generate a signal that can be detected by the sensor. Biosensors can be designed to detect various aspects of the virus, such as the presence of viral

## Chapter 03: High Sensitivity Refractive Index Sensor Based on Two-Dimensional Photonic Crystal for chikungunya virus.

---

particles, viral proteins, or antibodies produced in response to the virus. Biosensors have several advantages for virus detection, including high sensitivity, specificity, and speed, which make them a promising tool for the rapid and accurate diagnosis of Chikungunya virus infection [9]. Optical techniques are revolutionizing how biological questions can be addressed directly in the living cell. The optical techniques that inform on the changes in mechanical properties during the infection cycle.

The addition of photonic crystals to biosensors has enabled highly sensitive and facilitated the development of highly miniaturized biosensors that can be integrated into portable devices. Photonic crystals are periodic structures that can manipulate the propagation of light through a photonic bandgap, by creating point defects or cavities. Their sensitivity, specificity, and non-intrusiveness make optical techniques indispensable to generating high-fidelity data, significantly improving the tools available for future research into blood disease [10].

Several research on biosensors-based photonic crystals focuses to ameliorate the phc parameters such as sensitivity and quality factors.

**Tayoub** in Ref [11] propose a design for the diagnosis of malaria-infected red blood cells (RBCs) in the wavelength range of 1130-1860 nm for TM-polarized light, where a high sensitivity of 700 nm/RIU can be achieved.

**Sujit Kumari** in ref [12] design a biosensor structure to detect infected red blood cells by malaria parasites where the maximum sensitivity value obtained from his structure is 327.7 nm/RIU.

In our study we propose a two-dimensional phc waveguide as a biosensor to detect the infected blood component and uric acid by the chikungunya virus, we design and simulate a 2D photonic crystal biosensor. Where the biosensor chip is filled with a blood sample and urine and according to their refractive index transmission is deliberated. The software package OPTIFDTD and the 'PWE band solver' are used.

### 1. Article Structure and the Corresponding Styles

The proposed structure is based on hexagonally distributed air holes in a GaAs substrate, the refractive index of the GaAs material is 3.35 and the air is 1 where the radius of the holes and the lattice constant are 0.21  $\mu\text{m}$  and 0.6  $\mu\text{m}$  respectively. The figure shows the proposed design, the figure shows the 3D structure, and the parameter design is summarized



## Chapter 03: High Sensitivity Refractive Index Sensor Based on Two-Dimensional Photonic Crystal for chikungunya virus.

---

in the table.

Chapter 03: High Sensitivity Refractive Index Sensor Based on Two-Dimensional Photonic Crystal for chikungunya virus.

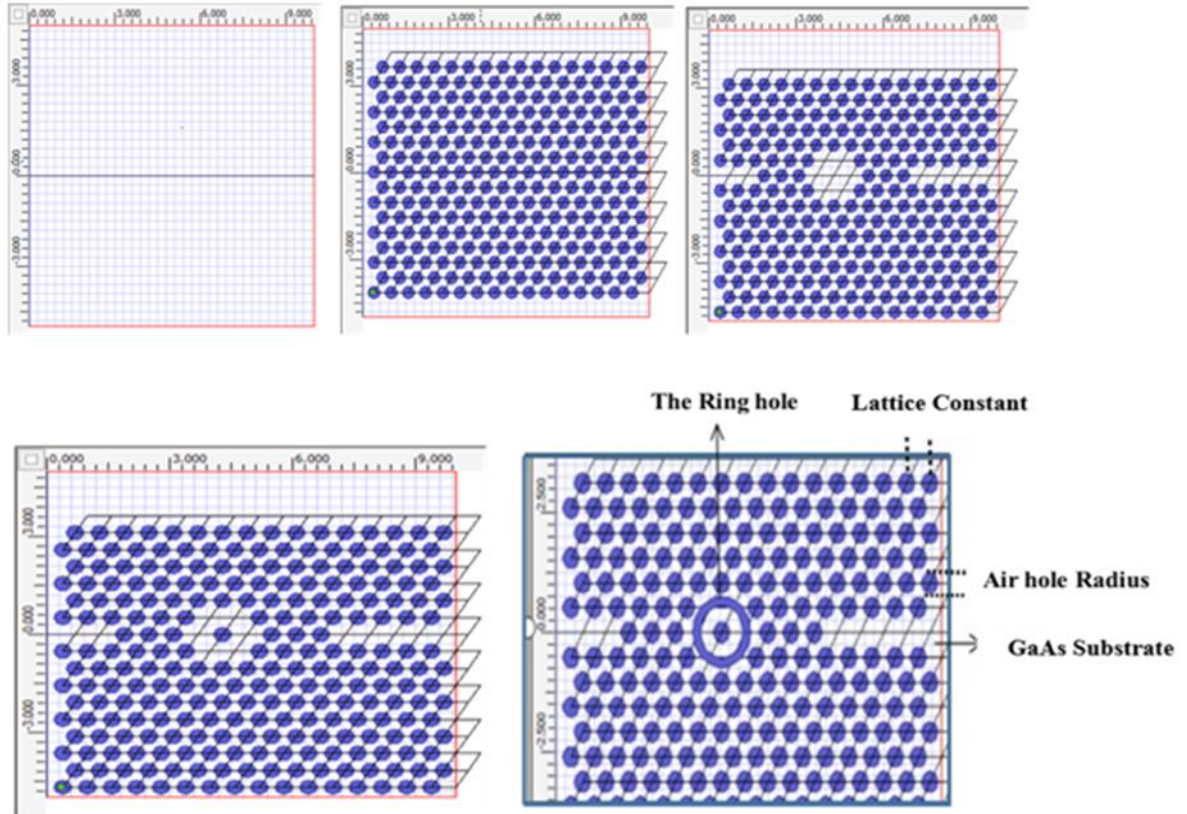


Figure 22 : The proposed design.

Formulaire 3d :

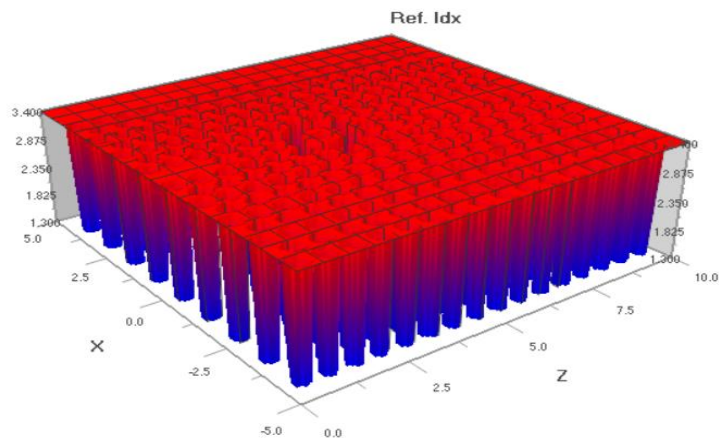


Figure 23 :The structure in 3D.

## Chapter 03: High Sensitivity Refractive Index Sensor Based on Two-Dimensional Photonic Crystal for chikungunya virus.

*Table 1 : Design Parameters.*

Design paramètre	The Value
Length*Width	17*16
The refractive index of GaAs	3.35
Hole radius	0.210 um
Lattice constant	0.6 um
The refractive index of the area	1
Ring width	0.65 um
Ring radius	0.2 um

The band gap of the photonic crystal structure has been calculated with the plane wave extension method (PWE) The complete structure has a certain range of wavelength in transverse electric mode from 2.078492 to 2.797416 $\mu$ m.

The results' bad gap was shown in Fig 24. The photonic crystal biosensor is excited from the light source by a Gaussian laser pulse with a central frequency of 2.31499 $\mu$ m and by applying an appropriate boundary condition (perfectly matched layer, PML). Fig 25 represents the distribution field.

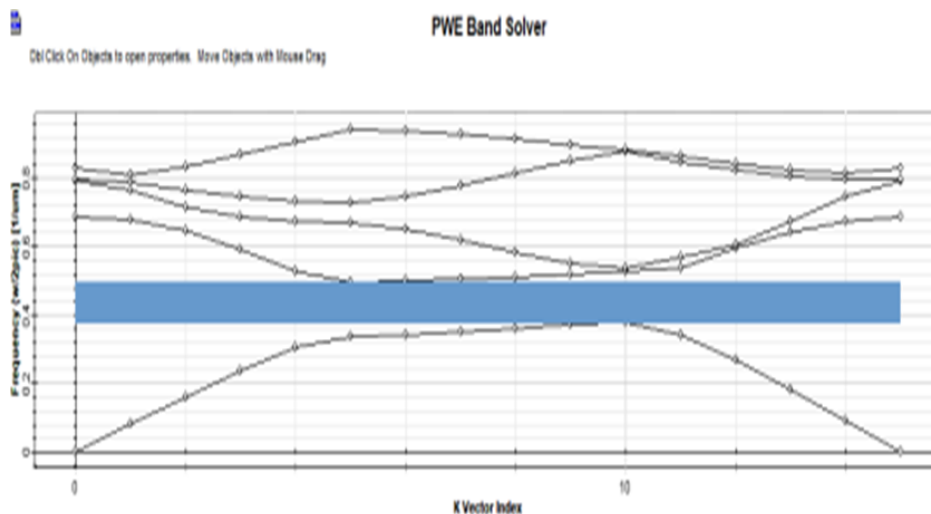


*Figure 24 : The band gap of the photonic crystal structure.*

## Chapter 03: High Sensitivity Refractive Index Sensor Based on Two-Dimensional Photonic Crystal for chikungunya virus.

---

The mid-infrared (MIR) region (about 2–20  $\mu\text{m}$ ) bears a particular scientific and technological significance due to a multitude of applications within diverse fields. And the major challenge in mid-IR sensing is the lack of efficient detectors [13].

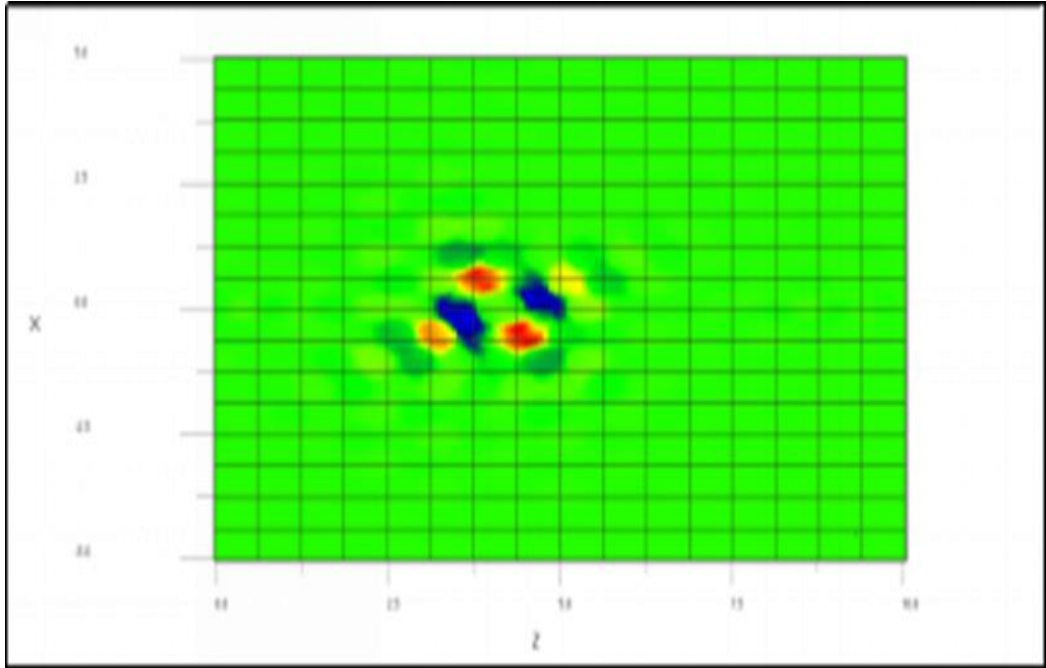


Figure 25 : Field distribution.

### 2. Geometric Study

In this section, we present 3 studies on the design structure:

In the first one, we change the radius of the annular hole from 0.4 to 0.65  $\mu\text{m}$  and in the second study we change the width of the annular hole from 0.27 to 0.35, and finally in the third one we change the radius of the central hole from 0.21 to 0.41  $\mu\text{m}$  and we calculate the sensitivity for each change. We limit our study to these values to avoid interference between pillars. Table 2 summarized the calculation results.

## Chapter 03: High Sensitivity Refractive Index Sensor Based on Two-Dimensional Photonic Crystal for chikungunya virus.

*Table 2 : Sensitivity value for each Parameter change.*

Change of		The sensitivity
The radius of the annular hole	Ra=0.4	377.115nm
	Ra=0.5	399.299 nm
	Ra=0.6	534.4nm
	R=0.65	475.117nm
The width of the annular hole	w=0.27	773.44nm
	w=0.30	499.123nm
	w=0.35	933.78nm
The radius of the central hole	Rc=0.21	475.117nm
	Rc=0.26	665.498nm
	Rc=0.31	737.474nm
	Rc=0.41	749.088nm

The curve in Fig 26 represents the change in the sensitivity according to the ring hole width where the highest sensitivity reached was 933.78nm/RIU at this point the width and the radius of the annular hole were 0.35 $\mu$ m, and 0.65 $\mu$ m respectively, and the central radius was 0.21 $\mu$ m. Fig 27 represents the final design.

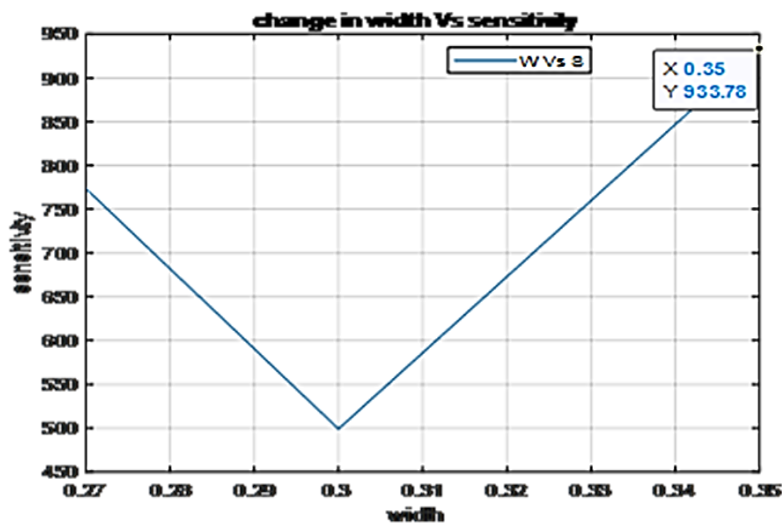


*Figure 26 : change in the width Vs the sensitivity.*

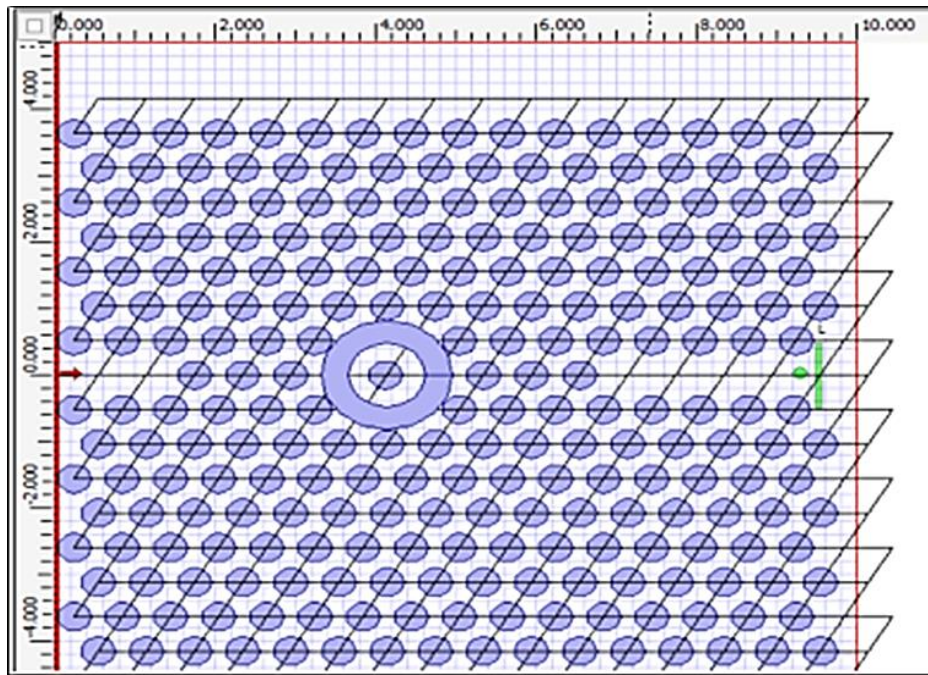


Figure 27 : The final design.

### 3. Discussion and Results

It appears in fig 26 that strong light is confined in the cavity, this localization of light increases after infiltration the interaction light-matter where a higher level of sensitivity can be reached.

We detect the normalized transmission spectrum after the infiltration of the structure of normal and infected blood components such as red blood cells, platelets, plasma, and also uric acid. All refractive indices of our samples are cited in the table3

The normalized transmission spectrum detected at the end of the structure by the photodetector looks like a lorentz pic, a shift in the wavelength of our pic between the infiltration by healthy and infected components was shown in fig 28-30

After infiltration of the design by the uric acid, another pic appears in fig 31, this phenomenon is called the fano resonance which is predominantly used to describe asymmetric resonance [14].


This fano resonance is sensitive to the small change in the environment's refractive index [15].

The sensitivity and the quality factor have been calculated for each detection shift. All results are summarized in the table3.

## Chapter 03: High Sensitivity Refractive Index Sensor Based on Two-Dimensional Photonic Crystal for chikungunya virus.

Table 3 : Refractive index of each analyte.

The target samples		Refractive index
RBC	Normal	1.4
	infected	1.39
Plasma	Normal	1.35
	infected	1.33
Platelets	Normal	1.39
	infected	1.38
uric acid	Normal	1.72
	infected	1.7

 Dbl Click On Objects to open properties. Move Objects with Mouse Drag

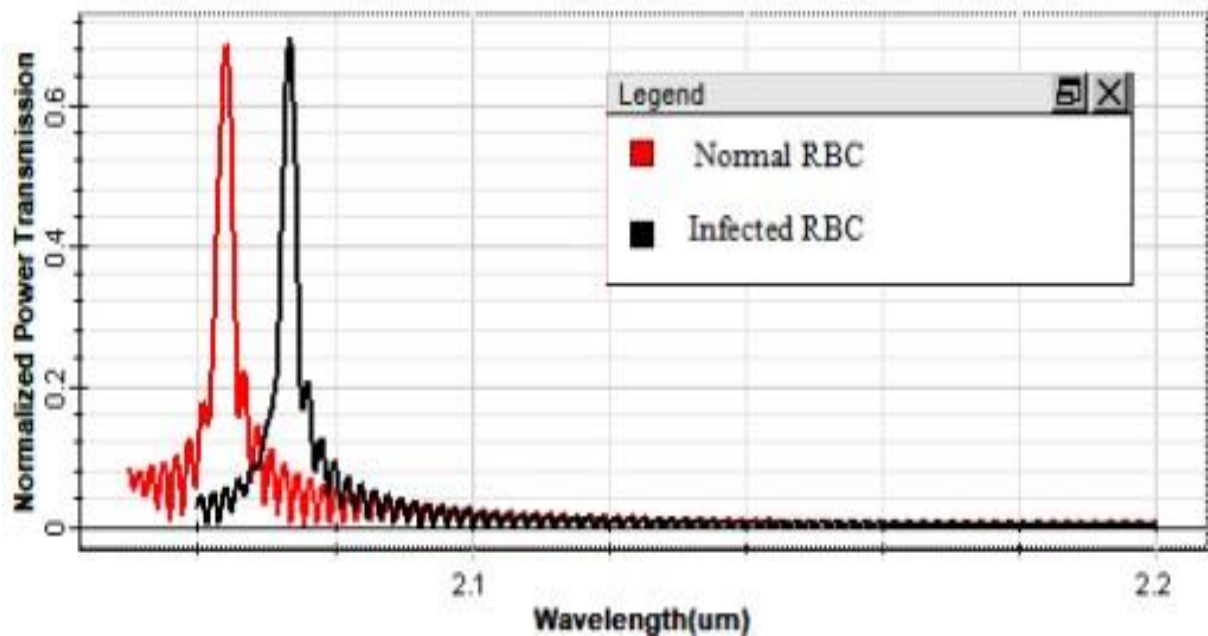


Figure 28 : Normalized transmission spectrum of healthy and infected RBC.

### Chapter 03: High Sensitivity Refractive Index Sensor Based on Two-Dimensional Photonic Crystal for chikungunya virus.

Dbt Click On Objects to open properties. Move Objects with Mouse Drag

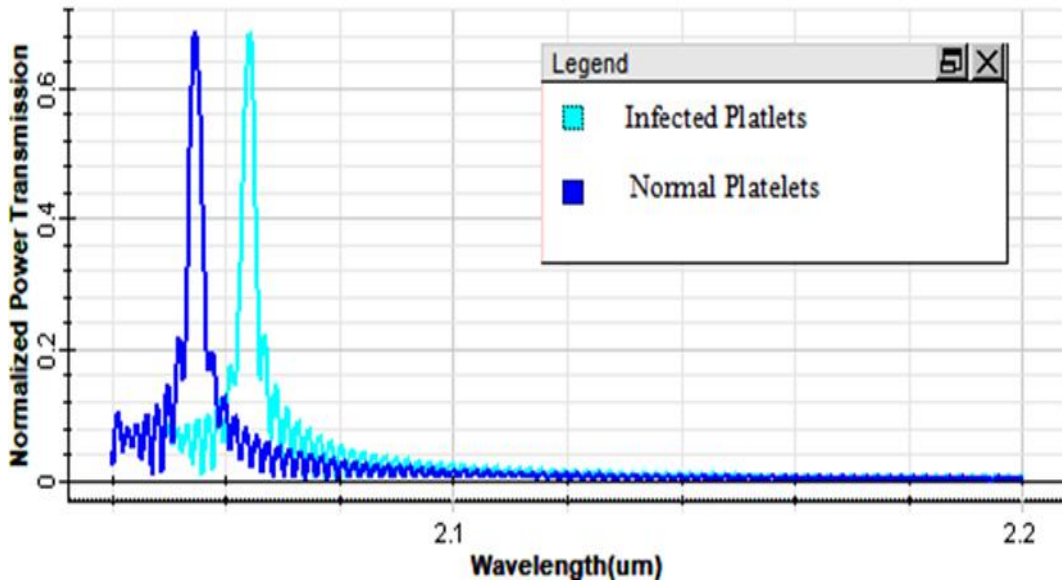


Figure 29 : Normalized transmission spectrum of healthy and infected Platelets.

Dbt Click On Objects to open properties. Move Objects with Mouse Drag

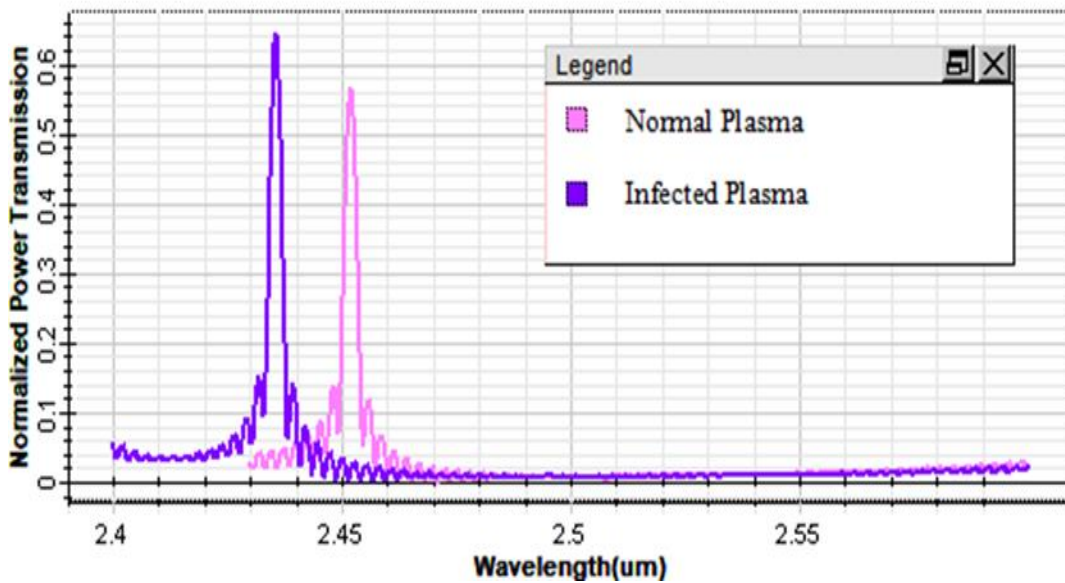


Figure 30 : Normalized transmission spectrum of healthy and infected plasma.



## Chapter 03: High Sensitivity Refractive Index Sensor Based on Two-Dimensional Photonic Crystal for chikungunya virus.

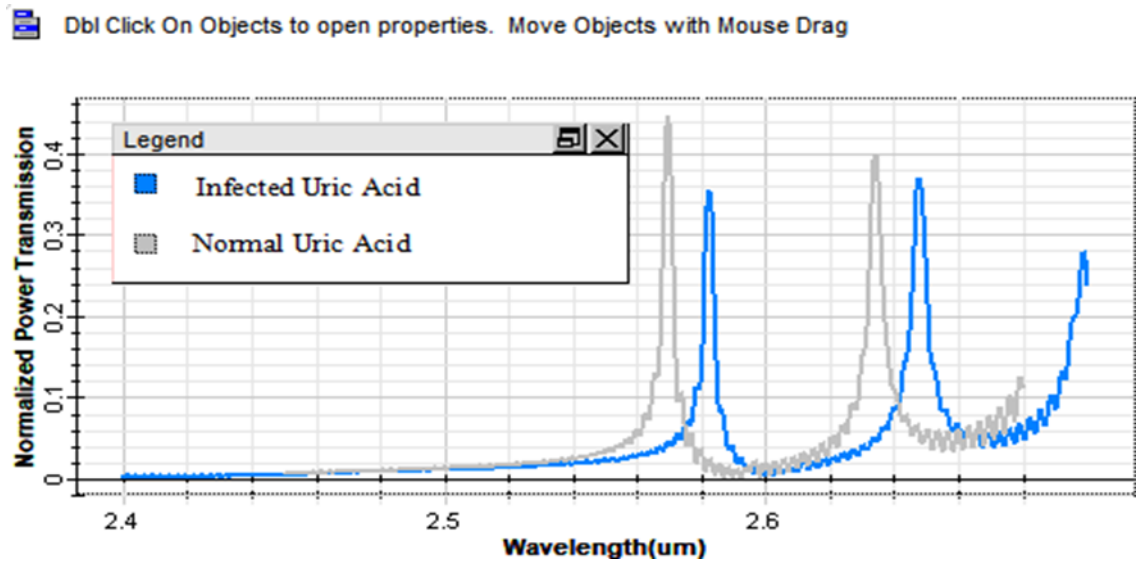


Figure 31 : Normalized transmission spectrum of healthy and infected uric acid.

Table 4 : Sensitivity, effectiveness, and quality factor for each analyte.

The analyte	The sensitivity	Quality factor	Transmission efficiency
Uric acid	665.12 nm/RIU	483.05	39.70%
platlets	973.24 nm	695.18	68.42%
Plasma	814.0 nm	727,59	64%
RBC	933.78 nm	778.61	69.2%

A

brief comparison

Comparison between our study and a few examples of other recent work has been presented in Table 5:

Table 5 : Comparison of Research.

Reference	Year	Structures	targeted Application	The sensitivity
[16]	2023	Basal_ MCF-7_ MDA-MB-231_ PC12_ HeLa_ Jurkat.	Label-Free cancer	308.5 (nm/RIU)
[17]	2023	Deionized water	bacterial water detection	232 nm/RIU
My work	2023	RBC_ Aside from urine	Chikungunya virus	973.24nm/RIU

## Conclusions

In this chapter, we have proposed a 2D photonic crystal structure biosensor to detect the influence of the chikungunya virus on blood components and uric acid. After a geometric study, we found a performance parameter that led to achieving a very high sensitivity of 973.24 um a transmission efficiency of 69.2%, and a quality factor of 778.61. Due to the importance of the accuracy and sensitivity parameters in the sensors' design, we can say that the achieved sensitivity compared to a recent work proves the value of our design.

## Bibliographic References

- [1] C. J. Puntasecca, C. H. King, and A. D. LaBeaud, 'Measuring the global burden of chikungunya and Zika viruses: A systematic review', *PLoS Negl. Trop. Dis.*, vol. 15, no. 3, p. e0009055, Mar. 2021, doi: 10.1371/journal.and.0009055.
- [2] R. Hussain, I. Alomar, and Z. A. Memish, 'Chikungunya virus: the emergence of an arthritic arbovirus in Jeddah, Saudi Arabia', *East. Mediterr. Health J.*, vol. 19, no. 5, pp. 506–508, May 2013, doi: 10.26719/2013.19.5.506.
- [3] S. Sunil, 'Current Status of Chikungunya in India', *Front. Microbiol.*, vol. 12, 2021, Accessed: Jun. 02, 2023. [Online]. Available: <https://www.frontiersin.org/articles/10.3389/fmicb.2021.695173>
- [4] M. Thakare, R. K. Bakshi, V. D. Sharma, K. M. Raul, and M. K. Doibale, 'Prospective Study of Clinical Features and Sequelae of Suspected Cases of Chikungunya Fever Admitted in Urban Areas of Central India', *Int. J. Health Sci.*, no. 5, 2017.
- [5] W. H. Organization, *Toolkit for Integrated Vector Management in Sub-Saharan Africa (A)*. World Health Organization, 2016.
- [6] P. Z. Xiaohuan Wang, 'Development of small-molecule viral inhibitors targeting various stages of the life cycle of emerging and re-emerging viruses', *Front. Med.*, vol. 11, no. 4, pp. 449–461, Dec. 2017, doi: 10.1007/s11684-017-0589-5.
- [7] Mohan A, Kiran D, Manohar I C, Kumar D P - Indian J Dermatol 'Epidemiology, clinical manifestations, and diagnosis of chikungunya fever: Lessons learned from the re-emerging epidemic'. <https://www.e-ijd.org/article.asp?issn=00195154;year=2010;volume=55;issue=1;spage=54;epage=63;aulast=Mohan>(accessed Jun. 02,2023).
- [8] Krauer F, Riesen M, Reveiz L, and al. Zika Virus Infection as a Cause of Congenital Brain Abnormalities and Guillain–Barré Syndrome: Systematic Review. *PLoS Med.* 2017; 14(1).doi:10.1371/journal.pmed.10022.
- [9] S. Sharma, A. Kumar, Kh. S. Singh, and H. K. Tyagi, '2D photonic crystal based biosensor for the detection of chikungunya virus', *Optik*, vol. 237, p. 166575, Jul. 2021, doi: 10.1016/j.ijleo.2021.166575.

- [10] J. M. A. Mauritz *et al.*, ‘Biophotonic techniques for the study of malaria-infected red blood cells’, *Med. Biol. Eng. Comput.*, vol. 48, no. 10, pp. 1055–1063, Oct. 2010, doi 10.1007/s11517-010-0668-0.
- [11] H. Tayoub, A. Hocini, and A. Harhouz, ‘High-Performance Two-Dimensional Photonic Crystal Biosensor to Diagnose Malaria Infected RBCs’, *Високоєфективний двовимірний фотонно-кристалічний біосенсор для діагностики еритроцитів, інфікованих малярією*, 2023, Accessed: Jun. 02, 2023. [Online]. Available: <https://essuir.sumdu.edu.ua/handle/123456789/91074>
- [12] S. K. Saini and S. K. Awasthi, ‘Sensing and Detection Capabilities of One-Dimensional Defective Photonic Crystal Suitable for Malaria Infection Diagnosis from Preliminary to Advanced Stage: Theoretical Study’, *Crystals*, vol. 13, no. 1, Art. no. 1, Jan. 2023, doi: 10.3390/cryst13010128.
- [13] Ashik A. S., Callum F. O’Donnell, S. Chaitanya Kumar, M. Ebrahim-Zadeh, P. Tidemand-Lichtenberg, and C. Pedersen, ‘Mid-infrared upconversion imaging using femtosecond pulses’, *Photon. Res.* 7, 783-791 (2019).
- [14] W. Zhou *et al.*, ‘Progress in 2D photonic crystal Fano resonance photonics’, *Prog. Quantum Electron.*, vol. 38, no. 1, pp. 1–74, Jan. 2014, doi: 10.1016/j.pquantelec.2014.01.001.
- [15] V. V. Klimov, A. A. Pavlov, I. V. Treshin, and I. V. Zabkov, ‘Fano resonances in a photonic crystal covered with a perforated gold film and its application to bio-sensing’, *J. Phys. Appl. Phys.*, vol. 50, no. 28, p. 285101, Jun. 2017, doi: 10.1088/1361-6463/aa75e6.
- [16] F. Baraty and S. Hamedi, ‘Label-Free cancer cell biosensor based on photonic crystal ring resonator’, *Results Phys.*, vol. 46, p. 106317, Mar. 2023, doi: 10.1016/j.rinp.2023.106317.
- [17] B. A. Kumar, S. K. Sahu, G. Palai, and I. Bala, ‘Modelling and performance analysis of ring resonator-based refractive-index sensor for bacterial water detection’, *Opt. Quantum Electron.*, vol. 55, no. 3, p. 263, Jan. 2023, doi: 10.1007/s11082-022-04507-9.

# **General Conclusion**

## General Conclusion

The aim of this work was the design and simulation of a photonic crystal biosensor to detect the chikungunya virus with high sensitivity. To achieve this goal we have followed the following steps:

- ❖ In the first step we talked about photonic crystals as a theory and a concept, then we looked at the use of such structures to develop detectors and sensors of different types and thus cover all the characteristics that lead to a high-performance sensor.
- ❖ In the second step, we explained how to work on the optiFDTD program and the simulated method using the Plane Wave-Expansion (PWE) method and the Finite-Difference Time-Domain (FDTD) algorithm.
- ❖ The last step of our work was to propose a structure, to define its characteristics (the lattice constant, the radius of holes  $r$ , the shape of the cavity, and the shapes of the waveguides included) and its optical GAP to define the wavelength range in which it must be exploited. Then this structure is optimized to obtain maximum sensitivity and good quality factors.

Thanks to the design we used, our results show a significant improvement in sensitivity compared to that found by ref [1] with its original structure. Our results show that RI sensitivity increased from 700 nm/RIU to 973.24um/RIU, which makes it very good support for the realization of a biosensor.

This sensitivity is very important and by comparing it with the literature in the field it has been found that it has a very competitive value.

In perspective, we encourage the PFEs of the promotions to come, to discover other designs for this sensor, and/or to do other optimization processes such as optimizing the layouts and lengths of the input and output waveguides to guarantee a better coupling between the source and the cavity and also to have a high sensitivity and a better quality factor.

## **Bibliographic References**

- [1] TAYOUB, H.; HOCINI, A.; HARHOUZ, A. High-Performance Two-Dimensional Photonic Crystal Biosensor to Diagnose Malaria Infected RBCs. *J. Nano- Electron. Phys.*, vol. 15, no. 1, pp. 01008-1-01008–6, 2023, doi: 10.21272/jnep.15(1).01008.